



## Global-regional nested simulation of particle number concentration by combing microphysical processes with an evolving organic aerosol module

5 Xueshun Chen<sup>1,3</sup>, Fangqun Yu<sup>6</sup>, Wenyi Yang<sup>1,3</sup>, Yele Sun<sup>1,2,3</sup>, Huansheng Chen<sup>1</sup>, Wei Du<sup>1,7</sup>, Jian Zhao<sup>1</sup>, Ying Wei<sup>1,4</sup>, Lianfang Wei<sup>1,3</sup>, Huiyun Du<sup>1</sup>, Zhe Wang<sup>1</sup>, Qizhong Wu<sup>5</sup>, Jie Li<sup>1,3</sup>, Junling An<sup>1,2</sup>, Zifa Wang<sup>1,2,3</sup>

<sup>1</sup>The State Key Laboratory of Atmospheric Boundary Layer Physics and Atmospheric  
10 Chemistry, Institute of Atmospheric Physics, Chinese Academy of Sciences, Beijing 100029, China

<sup>2</sup>College of Earth and Planetary Sciences, University of Chinese Academy of Sciences, Beijing 100049, China

<sup>3</sup>Center for Excellence in Regional Atmospheric Environment, Institute of Urban  
15 Environment, Chinese Academy of Sciences, Xiamen 361021, China

<sup>4</sup>Institute of Urban Meteorology, China Meteorology Administration, Beijing 100089, China

<sup>5</sup>College of Global Change and Earth System Science, Beijing Normal University, Beijing 100875, China

<sup>6</sup>Atmospheric Science Research Center, State University of New York at Albany, New York 12203, USA

<sup>7</sup>Institute for Atmospheric and Earth System Research/Physics, Faculty of Science, University of Helsinki, Helsinki 00014, Finland

25 *Correspondence to:* Zifa Wang (zifawang@mail.iap.ac.cn)

### Abstract

Aerosol microphysical processes are essential for the next generation of global and regional climate and air quality models to determine the particle size distribution.  
30 The contribution of organic aerosol (OA) to particle formation, mass and number concentration is one of the major uncertainties in current models. A new global-regional nested aerosol model was developed to simulate detailed microphysical processes. The model combined an advanced particle microphysics (APM) module and a volatility basis-set (VBS) organic aerosol module to calculate



35 the kinetic condensation of low volatile organic compounds and equilibrium  
partitioning of semi-volatile organic compounds in a 3-dimensional (3-D) framework  
using global-regional nested domain. In addition to the condensation of sulfuric acid,  
equilibrium partitioning of nitrate and ammonium, and the coagulation process of  
particles, the microphysical processes of the organic aerosols are realistically  
40 represented in our new model. The model uses high-resolution size-bins to calculate  
the size distribution of new particles formed through nucleation and subsequent  
growth. The multi-scale nesting allows the model to use high resolution to simulate  
the particle formation processes in the urban atmosphere in the background of  
regional and global environments. Using the nested domains, the model reasonably  
45 reproduced the OA components from analysis of Aerosol Mass Spectrometry (AMS)  
measurements by Positive Matrix Factorization (PMF) and the particle number size  
distribution (PNSD) in Megacity Beijing during a period of about a month.  
Anthropogenic organic species accounted for 67% of the OA of secondary particles  
formed by nucleation and subsequent growth, significantly larger than that of biogenic  
50 OA. Over the global scale, the model well predicted the particle number concentration  
in various environments. The microphysical module combined with VBS simulated  
the universal distribution of organic components among the different aerosol  
populations. Model results strongly suggest the importance of anthropogenic organic  
species in aerosol particle formation and growth at polluted urban sites and over the  
55 whole globe under the influence of anthropogenic source areas.

**Key words:** IAP-AACM+APM, VBS, organic aerosol, particle number concentration

## 1Introduction

The increased concentrations of atmospheric aerosol particles caused by  
anthropogenic activities have become an important scientific issue due to their  
60 significant climate forcing and health effects (Twomey, 1977; Albrecht, 1989;  
Charlson et al., 1992; Donaldson et al., 2002; Tsigaridis et al., 2006; IPCC, 2013) in  
global and regional scales. These effects depend on aerosol size, composition, and  
mixing state. The direct influence of aerosols on climate is their scattering of solar  
radiations largely determined by the key properties of aerosols mentioned above



65 (IPCC, 2013). The indirect effects of aerosols are driven by their ability in affecting  
cloud microphysical properties and precipitation processes through serving as cloud  
condensation nuclei (CCN), which is highly dependent on CCN number  
concentrations (Dusek et al., 2006). Ultrafine particles, though having lower mass  
concentration, have larger health effect due to their easier penetration and higher  
70 number concentrations (Delfino et al., 2005; Kumar et al., 2014). Therefore, it is  
crucial to gain deep insight into the life cycle of aerosol particles and quantify their  
sources not only in mass concentration but also in their number concentration.

There are two sources of atmospheric aerosols: direct emissions from primary  
sources and secondary formation processes (Seinfeld and Pandis, 2006). Mineral dust  
75 particles over desert regions and sea salt particles over oceans are the two major  
natural sources contributing to the particle mass and number concentration regionally  
(Textor et al., 2006). Anthropogenic activities, such as fossil fuel combustion and  
biomass burning, can directly emit particles and they are the most significant  
contributors to the aerosols since the industrial revolution (IPCC, 2013). The physical  
80 and chemical properties of these primarily emitted particles can be modified by  
condensation, coagulation, and chemical reactions in the atmosphere (Seinfeld and  
Pandis, 2006). In addition, new particle formation (NPF) is found to be an important  
contributor to aerosol particles in global various environments (Holmes, 2007; Yu et  
al., 2008; Yu and Luo, 2009; Kulmala et al., 2013). Field observation studies also have  
85 demonstrated that the new particle formation can significantly increase CCN number  
concentrations (Kuang et al., 2009; Wiedensohler et al., 2009; Yue et al., 2011). It is  
necessary to reasonably represent primary emission, their microphysical aging, and  
new particle formation process in 3-D models.

During the past two decades, there has been numerous models incorporating  
90 microphysical module to describe the particle formation processes (e.g., Binkowski  
and Shankar, 1995; Jacobson, 1997; Stier et al., 2005; Bergman et al., 2012). However,  
large uncertainties still exist due to the complication of processes and the mechanisms  
not well understood. Intercomparison and evaluation of global aerosol models indicate  
that constraint of size-resolved primary emission and improved understanding of



95 secondary formations are required to improve the ability of model in simulating  
particle number size distribution (Mann et al., 2014). Spracklen et al. (2005) find that  
the assumption of the size distribution has a large impact on particle number  
concentrations in the boundary layer. The comparison between the simulation and the  
Single Particle Soot Photometer (SP2) measurements suggests that the model has  
100 large bias in simulating the number size distribution of black carbon particles  
(Reddington et al., 2013). Significant improvements in the simulation of the particle  
number concentration and aerosol optical properties were achieved by using an  
optimized size distribution of primary particles in polluted atmosphere over areas with  
large emissions (Zhou et al., 2012, 2018). Much work remains to reduce the  
105 uncertainty associated with primary emissions, especially over primary particles  
dominated regions in terms of particle number concentration, like China.

The main source of uncertainty in simulating new particle formation at regional  
and global scales can be attributed to the nucleation mechanism and particle growth  
rates unexplained. Although sulfuric acid has been identified as a major component  
110 and plays a central role in nucleation (Yu and Turco, 2001; Boy et al., 2005; Kirkby et  
al., 2011), alone it could not explain the new particle formation rates (Wang et al.,  
2013; Kulmala et al., 2013). Recent studies revealed that certain organic vapors are  
involved in the particle nucleation (Metzger et al., 2010; Zhang et al., 2012; Yao et al.,  
2018) and contribute much to the particle growth (Kulmala and Kerminen, 2008;  
115 Tröstl et al., 2016). It is no doubt that reasonable representation of organic aerosol  
(OA) is crucial for aerosol models to realistically simulate new particle formation and  
growth. However, it is still an open question which organic species are possibly  
involved in new particle formation process. Even the chemical composition and the  
sources of OA are still uncertain as they contain large number of compounds  
120 (Goldstein and Galbally, 2007). Up to now, OA is still the least understood one  
among the components of aerosols (Kanakidou et al., 2005; Hallquist et al., 2009).  
Clearly, the OA representation is the major uncertainty contributing to the huge gap in  
elucidate particle formation processes.

In recent years, much progress has been achieved in simulating the formation of



125 OA and secondary organic aerosol (SOA). The two product (2P) model recommended  
by Odum et al. (1996) had been widely used in 3-D models to describe SOA  
formation process empirically. The volatility basis-set (VBS) approach was recently  
developed to represent the oxidation of primary OA (POA) and SOA and the  
partitioning of OA in different volatilities between gas phase and aerosol phase  
130 (Donahue et al., 2006). Many regional models have used VBS to simulated OA and  
SOA (Shrivastava et al., 2008; Fountoukis et al., 2011; Ahmadov et al., 2012; Zhao et  
al., 2016; Han et al., 2016). However, application of VBS in global models is limited  
for the large number of tracers required and the uncertainty of the involved parameters  
(Farina et al., 2010; Hodzic et al., 2016). There are even fewer applications of this  
135 unified framework in 3-D global aerosol models to calculate the processes of particle  
formation. Among the second phase AeroCom aerosol microphysical models,  
simplified parameterization and two-product method are the mostly used schemes to  
represent SOA (Mann et al., 2014). Recently, there has been some models with VBS  
incorporated in their microphysical module to simulate aerosol microphysical  
140 formation process. Patoulias et al. (2015) developed a new aerosol dynamics model  
with VBS and explored the contribution of SOA with different volatility to particle  
growth in different stages, but the 3-D modeling was not presented. By assuming  
equilibrium partitioning for all volatility bins, Gao et al. (2017) implemented VBS in  
an aerosol microphysics model and examined the effect of semi-volatile SOA on the  
145 composition, growth, and mixing state of particles. Their simulation of box model  
suggested that the volatility of organic compounds simulate rather different mixing  
states from those simulated by coagulation process alone in the scheme treating  
primary emission of organics as nonvolatile. Matsui (2017) represented aerosol size  
distribution with a two-dimensional sectional method in a global aerosol model  
150 coupled with the VBS scheme, but the size-bin resolution is not high enough to well  
resolve the growth of new particles.

To our knowledge, there is currently scarce 3-D modeling study using VBS to  
account for both (1) the kinetic condensation of low-volatile organics and  
re-evaporation of semi-volatile organics and (2) the size-resolved kinetics of the mass



155 transfer for new particles. In addition, the particle formation in the polluted  
atmosphere was not well understood (Kulmala et al., 2016; Wang et al., 2017; Chu et  
al., 2019). Over the urban areas in northern China, observation and modeling studies  
indicate that anthropogenic SOA contributes a larger fraction to OA than that of  
biogenic one and play an significant role in particle formation (Yang et al., 2016; Guo  
160 et al., 2020; Han et al., 2016; Lin et al., 2016). Simultaneously calculating both  
anthropogenic and biogenic SOA in microphysical models with high resolution is  
crucial to resolve the particle formation processes over the urban areas. Furthermore,  
the previous studies focusing on the sensitivity of particle number concentration to  
primary emission were based on models without considering the detailed  
165 microphysics of organic species (e.g., Spracklen et al., 2006; Chang et al., 2009; Chen  
et al., 2018; Zhou et al., 2018). Therefore, it is urgently needed to establish a 3-D  
modeling framework of VBS with an aerosol microphysics module with high size-bin  
resolution to simulate the particle number size distribution and explore the  
uncertainties associated with the treatment of primary emission.

170 In our previous work, a regional model with detailed microphysical processes  
has been developed to improve the new particle formation in summer in Beijing  
(Chen et al., 2019). In this study, we extend our work to the global scale and doing so  
to establish a new aerosol model by coupling a VBS organic aerosol scheme with a  
particle microphysics module in a global-regional nested model. The model  
175 performance was evaluated against the measurements at a tower and the collected  
dataset from published papers. In addition, the model's sensitivity to the size  
distribution of primary emission and volatility distribution of POA are explored to  
understand and quantify the uncertainties associated. The new modeling framework  
can provide a useful tool to simulate aerosol microphysical process in both global and  
180 regional scales. The description of model and its development method are introduced  
in Sect.2. The experiments setup and model input are detailed in Sect.3. The observed  
data used for evaluating model performance are described in Sect.4. The model results  
and simulation analysis are presented in Sect.5. The conclusions and discussions are  
summarized in Sect.6.



## 185 **2 Model description**

### **2.1 Host model**

The host model employed in this study is the Atmospheric Aerosol and Chemistry Model developed by Institute of Atmospheric Physics, Chinese Academy of Sciences (IAP-AACM). The IAP-AACM is a 3-D atmospheric chemical transport  
190 model treating chemical and physical processes for gases and aerosols in global and regional scales using multi-scale domain-nesting technique (Wang et al., 2001; Li et al., 2012; Chen et al., 2015). The model has been successfully used to explore mercury transport (Chen et al., 2015) and simulate the global and regional distribution of gaseous pollutants, aerosol components (Du et al., 2019; Wei et al., 2019). The  
195 calculation of some modules in the model has also been optimized recently (Wang et al., 2017, 2019). The model calculates 3-D advection (Walcek, 1998), turbulent diffusion (Byun and Dennis, 1995), gas phase chemical reactions (Zaveri and Peters, 1999), dry deposition at the surface (Zhang et al., 2003), aqueous reactions in the cloud and wet scavenging (Stockwell et al., 1990), and heterogeneous chemical  
200 process (Li et al., 2012). The partition of nitric acid and ammonia into particle phase to form nitrate and ammonium are simulated using a thermodynamic equilibrium model (Nenes et al., 1998). The model calculates the online emission of dimethyl sulfide (DMS) (Lana et al., 2011), sea salt (Athanasopoulou et al., 2008) and dust (Wang et al., 2000; Luo and Wang, 2006). The simulation results of IAP-AACM have  
205 been evaluated against a comprehensive observation dataset and compared with other model results. The model showed good performance in reproducing global aerosol components (Wei et al., 2019).

### **2.2 APM module**

Advanced Particle Microphysics (APM) module is an aerosol module using the  
210 sectional method to represent particle number size distribution. APM has been coupled to several 3-D models, such as GEOS-Chem (Yu and Luo, 2009), WRF-Chem (Luo and Yu, 2011), and NAQPMS (Chen et al., 2014). In APM, there are two types of aerosol particles: one is secondary particles (SPs) and the other is primary particles (PPs) with a secondary species coating. The definitions of SPs and



215 PPs in our model are different from secondary aerosol and primary aerosol commonly  
used in the community. SPs indicate their source is the nucleation and the subsequent  
growth of newly nucleated particles whereas PPs are from the direct emission. PPs  
include dust particles, sea salt particles, organic carbon (OC) particles, and black  
carbon (BC) particles. The APM has a high size-bin resolution to accurately describe  
220 the formation and growth processes of SPs (composed of sulfate, nitrate, ammonium,  
and organic compounds). SPs are represented by 40 size bins from 0.0012  $\mu\text{m}$  to 12  
 $\mu\text{m}$  in dry diameter. Among the PPs, representation of BC and OC are updated from a  
modal method in the original version (Yu and Luo, 2009) to a size-bin scheme in the  
revised version (Chen, 2015). Dust particles in 0.03–50  $\mu\text{m}$  are represented by 4 size  
225 bins and sea salt particles in 0.0012–12  $\mu\text{m}$  are represented by 20 size bins. SPs are  
assumed to be internally mixed and PPs are assumed to be consisted of a primary core  
and coating species. SPs and PPs of different categories are externally mixed with  
each other. In addition to the primary core, the coated species are explicitly simulated  
in APM.

230 The basic microphysical processes in APM include nucleation,  
condensation/evaporation, coagulation, and thermodynamic equilibrium partition. The  
nucleation scheme is the ion-mediated nucleation (IMN) (Yu, 2006, 2010)  
physically-based and constrained by laboratory data, which have predicted reasonable  
distributions of global nucleation (Yu et al., 2008). Due to very low saturation vapor  
235 pressure, the condensation of  $\text{H}_2\text{SO}_4$  is explicitly calculated. The semi-volatile  
inorganic species (nitrate and ammonium) and secondary organic species are  
simulated through equilibrium partitioning. The bulk mass concentrations of coating  
species are tracked to reduce the computational cost and the corresponding tracers  
used are defined as BC sulfate, OC sulfate, sea salt sulfate, and dust sulfate,  
240 respectively. For coagulation, APM not only calculates the self-coagulation of sea salt  
particles, BC particles, OC particles, and SPs, and but also considers the coagulation  
scavenging of SPs by four types of PPs. Yu (2011) has further developed APM to  
explicitly calculate the co-condensation of sulfuric acid and low-volatility secondary  
organics gas (LV-SOG) on the secondary and primary particles. In the scheme, the



245 production rate of LV-SOG and the semi-volatile OA input to APM are simulated with  
the extended two-product SOA formation model. For high calculation efficiency, a  
pre-calculated look-up table of coagulation kernels is used in the coagulation module.  
The numerical scheme used is from Jacobson et al. (1994). More details on  
microphysical processes of APM can be found in the study of Yu and Luo (2009).

### 250 **2.3 VBS module**

To reproduce the formation and evolution of OA, a 1.5-D VBS approach (Koo et  
al., 2014) based on 1-D VBS framework but accounting for changes in the oxidation  
state and volatility of OA in the 2-D VBS space is coupled to the model. Both  
secondary and primary organic aerosols are distributed in five volatility bins ranging  
255 from  $10^{-1}$  to  $10^3 \mu\text{g}/\text{m}^3$  in saturation concentration ( $C^*$ ) at 298 K, and temperature  
dependence of  $C^*$  is calculated by the Clausius-Clapeyron equation (Sheehan and  
Bowman, 2001). The compounds distributed in the lowest bin with  $C^*$  less than  $10^{-1}$   
 $\mu\text{g}/\text{m}^3$  represents the effectively nonvolatile OAs and they are considered as  
low-volatile organic compounds almost partitioned to the particulate phase in our  
260 model. The compounds in other four bins, i.e.,  $C^* = \{10^0, 10^1, 10^2, 10^3\} \mu\text{g}/\text{m}^3$ , are  
defined as semi-volatile organic compounds that can be partitioned between the gas  
and particulate phase by equilibrium assumption (Donahue et al., 2009). To track the  
oxidation state of OA, four basis sets are used in the scheme: two-basis sets for  
chemically aged OA from anthropogenic and biogenic sources, and two-basis sets for  
265 freshly emitted OA from anthropogenic sources and biomass burning. The molecular  
properties for primary OA (POA) and SOA in each volatility bins are provided by the  
parameters calculated by 2-D volatility scheme (Donahue et al., 2011, 2012).

In this VBS module, gas phase organic compounds can be aged by extremely  
reactive hydroxyl radicals (OH) and other oxidants. Volatile organic precursors of  
270 SOA in this study include compounds with terminal olefin carbon bond ( $\text{R}-\text{C}=\text{C}$ ),  
internal olefin carbon bond ( $\text{R}-\text{C}=\text{C}-\text{R}$ ). The associated species in the model are  
terpenes, isoprene, and aromatics. Aging of POA by OH is at a reaction rate of  
 $4 \times 10^{-11} \text{cm}^3 \cdot \text{molecule}^{-1} \cdot \text{s}^{-1}$  (Robinson et al., 2007). In the calculation, a conception of  
“partial conversion” is used, i.e., the oxidation products are a mixture of POA and



275 oxidized POA (OPOA) in the adjacent lower volatility bins (Koo et al., 2014). In  
addition, the multigenerational oxidation processes of intermediate VOCs (IVOCs)  
with OH radicals at a rate constant of  $4 \times 10^{-11} \text{ cm}^3 \cdot \text{molecule}^{-1} \cdot \text{s}^{-1}$  are taken into account  
in SOA formation. IVOCs emission was put into the bin of  $10^4 \mu\text{g}/\text{m}^3$  saturation  
concentration. The VBS module in this study does not consider OA formation through  
280 aqueous-phase/heterogeneous reactions although their importance is suggested in  
some studies (e.g., Liu et al., 2012; Ervens et al., 2014; Lin et al., 2014). SOA  
generated from VOCs and IVOCs and anthropogenic OPOA are assumed to be further  
oxidized by OH radical at an aging rate of  $2 \times 10^{-11} \text{ cm}^3 \cdot \text{molecule}^{-1} \cdot \text{s}^{-1}$  based on the  
work in Koo et al. (2014). The volatilities of multi-generation oxidation products  
285 decrease and move down to the adjacent bin with an order of magnitude lower  
volatility (Donahue et al., 2006). The model has 32 pairs of semi-volatile compounds  
including organic gases (OGs) and the corresponding OAs through equilibrium  
partitioning. Plus the 8 groups of low-volatility OAs, the model has 40 groups of OAs  
and 32 groups of OGs in total. Detailed information on this VBS module can be found  
290 in Koo et al. (2014) and Yang et al. (2019).

#### 2.4 Model development

In our previous work, the VBS module has been combined with APM to improve  
the simulation on new particle formation process in our regional model  
(NAQPMS+APM, Chen et al., 2019). Here, we use the similar method to couple the  
295 VBS and APM into the global model, i.e., IAP-AACM. The newly developed model  
is named IAP-AACM+APM. In the model, not only the basic microphysical  
processes aforementioned but also the condensation of LV-SOG and equilibrium  
partition of semi-volatile OA (SV-OA) are calculated following the approaches  
described in Yu and Luo (2009) and Yu (2011). In addition to the tracers of OAs and  
300 OGs mentioned above, a new tracer for LV-SOG is tracked in IAP-AACM+APM. The  
sources of sulfuric acid and LV-SOG are photochemical reactions. Their production  
rates are calculated by CBM-Z and VBS module, respectively. The production rate of  
LV-SOG is equivalent to that of the lowest bin OAs in VBS module. For simplicity  
and computing efficiency, the condensation of LV-SOG on SPs of different sizes is



305 calculated along with  $\text{H}_2\text{SO}_4$  and the low volatile SOA (LV-SOA) on SPs are merged  
into one bulk tracer (SP-LV). When necessary, SP-LV is redistributed to size-bins  
according to the surface area of particles. The condensation of LV-SOG on PPs (i.e.,  
dust, sea salt, BC, and OC particles) is calculated in the same way as  $\text{H}_2\text{SO}_4$ . The  
amount of LV-SOA coated on these particles are defined as dust-LV, salt-LV, BC-LV  
310 and OC-LV. In this way, LV-SOAs are distributed approximately proportional to the  
aerosol surface area. The semi-volatile SOA (SV-SOA) partitioned to SPs in each bin  
and the coatings on PPs are assumed to be proportional to the corresponding LV-OA  
mass. For OC particles, the coated SV-SOA depends on both OC-LV and POC. The  
SV-SOA input to APM is the total mass concentration of 32 groups of semi-volatile  
315 OAs in VBS module. The partition of this part of OA is similar with that of  
equilibrium partition theory (Pankow, 1994a,b; Odum et al., 1996). By using the  
treatments above, the different microphysical behaviors of OAs with different  
volatilities are reasonably simulated. The dry deposition at the surface level and wet  
deposition by precipitation of LV-SOG are modeled using same scheme as  $\text{H}_2\text{SO}_4$ .  
320 The dry deposition and wet scavenging of the coated LV-OA associated with SPs and  
PPs are calculated using the same scheme as the sulfate coated on PPs (Yu, 2011).

The tracers associated aerosol microphysical processes in IAP-AACM+APM are  
listed in Table 1. The number of newly added tracers in IAP-AACM+APM is 129  
compared to IAP-AACM; and therefore, the computing time of 3-D advection and  
325 turbulent diffusion is nearly doubled comparing to IAP-AACM. Among the modules  
in IAP-AACM+APM, gas phase reaction module and the microphysical module are  
most time-consuming. The newly-developed processes in IAP-AACM+APM do not  
add much computing time. The total computing time of IAP-AACM+APM is less  
than that twice of IAP-AACM and it is acceptable. The aerosol microphysical module  
330 combining VBS with APM in this study can be used in other 3-D models.

### 3 Model configuration and experiments setting

#### 3.1 Model domain and model inputs

In this study, we use two nested modeling domains for one-year simulation in  
2010, with the first domain covering whole globe at 1 degree resolution, the second



335 domain covering east Asia at 0.33 degree resolution. The model has 20 vertical layers  
and the top layer is at 20 km. The simulation from December 1<sup>st</sup>, 2009 to December  
31<sup>st</sup>, 2010 was used for annual mean analysis and the first 1-month of simulation was  
spin-up time and not used in analysis. In addition, a case study in 2015 using three  
nested domains with the third domain of 0.11 degree resolution was conducted to  
340 evaluate the model performance in simulating OA components and particle number  
size distribution at a typical urban site. The model domains are shown in Fig.S1.

The meteorological parameters input to IAP-AACM+APM were simulated by  
the global version of Weather Research and Forecasting (WRF) model (Skamarock et  
al., 2008). The initial and boundary conditions of WRF was provided by Final  
345 Analysis (FNL) datasets from the National Centers for Environmental Prediction  
(NCEP) (<https://rda.ucar.edu/datasets/ds083.2>). The temperature, humidity, wind  
speed, and pressure in WRF were nudged to FNL datasets. Gridded emission  
inventory used in IAP-AACM+APM was an integrated dataset from a publicly  
datasets ([https://edgar.jrc.ec.europa.eu/htap\\_v2/index.php](https://edgar.jrc.ec.europa.eu/htap_v2/index.php)) and the multi-resolution  
350 emission inventory for China (MEIC) (<http://www.meicmodel.org>).

### 3.2 Experiments setting

One base experiment and four sensitivity experiments are used in our study. The  
sensitivity experiments involving size distribution of primarily emitted particles,  
including BC and POC, and the volatility distribution of POA, are designed to  
355 investigate the impact of these factors on the particle number concentration. Table 2  
lists the experiments used in this study. In the BASE experiment, the volatility  
distributions of POA from vehicles and biomass burning are based on the chamber  
studies (May et al., 2013a,b,c); the factors of other POA emissions are from the  
estimation of Robinson et al. (2007). In the LV\_POA and HV\_POA experiment,  
360 quartiles of the above mentioned distribution factors are used. In the OCD0.5 and  
PPD0.5 experiment, the geometric mean diameter is set half as the ones used in BASE  
experiment for POC, both BC and POC, respectively.

### 4 Observation data

The hourly observation of OA and particle number size distribution (PNSD) in



365 Beijing is used to evaluate the model performance in the typical urban environment. The observation site is located at the Tower Branch of the Institute of Atmospheric Physics (IAP), Chinese Academy of Sciences (CAS) (39°58'N, 116°22'E). The details of the observation site were described in Sun et al. (2015). The observation period was from 22 August to 30 September, 2015. Organics aerosol compositions were  
370 measured by a high-resolution aerosol mass spectrometer (HR-AMS, Aerodyne Research Inc.) and an aerosol chemical speciation monitor (ACSM, Aerodyne Research Inc.) at ground level and 260 m, respectively (Zhao et al., 2017). Using positive matrix factorization (PMF) algorithm (Paatero and Tapper, 1994; Paatero, 1997), organic aerosol (OA) were separated into hydrocarbon-like OA (HOA) and  
375 oxygenated OA (OOA). The detailed evaluation of PMF results was given in Zhao et al. (2017). PNSD from 15 to 685 nm at ground level and 260m on the 325m meteorological tower were measured by using two scanning mobility particle sizers (SMPSs). More details on the observation can be found in the published paper (Du et al., 2017). In model evaluation, the observed PNSD were mapped to the defined size  
380 bins of SPs in APM. OC concentrations in 2010 from the Interagency Monitoring of Protected Visual Environments (IMPROVE) network (<http://vista.cira.colostate.edu/improve>) and the China Atmosphere Watch Network (CAWNET) reported by Zhang et al. (2008) were used to compare with the simulated OC of our model. In addition, a list of surface observations of particle number  
385 concentration having at least one full year measurements was compiled to check model performance. Table S1 gives the compiled mean concentrations of condensation nuclei larger than 10 nm (CN10) and the corresponding station information from published papers.

## 5 Results

### 390 5.1 PNSD and aerosol components of SPs in Beijing

The simulated OA concentration is compared with the results of the PMF analysis of the AMS measurements before evaluating the simulated PNSD in Beijing. Here, HOA and OOA components by the PMF analysis have been compared with the simulation assuming they are primary and secondary components of OA, i.e., POA



395 and SOA, respectively. Affected by local emission sources (e.g., traffic emission and cooking emission), the observed values of OA were not representative at the ground level. Therefore, only HOA and OOA at the height of 260 m were used for comparison. The third-domain results at 0.11 degree horizontal resolution with the other configurations same with the base experiment were extracted for the analysis and comparison. First, BC simulations were compared with the observations (shown in Fig.1a), considering that BC is a passive tracer and it is generally co-emitted with POA. Since BC is only influenced by emissions, transport and deposition, the agreement between model and observations in Fig.1a suggests the model represented these processes reasonably well. Fig.1b and 1c show the comparison of the simulated and the observed hourly OA components at the 260m height. The comparison in Fig.1 highlights the good skill of model in capturing the variation of POA and SOA in our 3-D framework with VBS. Although the measurements at higher level were not susceptible to local emissions, the observed OA concentrations were inevitably influenced by the sources near the measurement site. For example, cooking emitted OA, assumed as a part of HOA here, have been identified as an important contributor to OA (Zhao et al., 2017). Moreover, the nearby traffic emissions would have large influences on the observed OA concentrations at the measurement site (Sun et al., 2015). Same as BC, the temporal variation of POA was mainly influenced by emissions, transport and deposition, the disagreement between the simulated POA and the observed HOA can largely be attributed to the emissions. In additions, the PMF analysis has its own uncertainties and deficiencies (Ulbrich et al., 2009). As a result, some observed values of HOA were not reproduced by IAP-AACM+APM. By contrast, most of the predicted SOA and their temporal variation were consistent with the observation of OOA although their concentrations were partially underestimated and some peaks were high. The correlation coefficient between the simulated SOA and observed OOA was 0.52. Overall, our model well simulated the POA and SOA concentrations.

400  
405  
410  
415  
420

During the past decades, many field observations have been conducted to study the characteristics of PNSD in Beijing (Wehner et al., 2004; Wu et al., 2007, 2008;



425 Wang et al., 2015). The NAQPMS model has been used to explain the evolution of  
PNSD in winter in Beijing (Chen et al., 2017). However, 3-D modeling study on these  
issues are still limited (Kulmala et al., 2016; Wang et al., 2016). Here, the observed  
PNSD at 260m height is used to evaluate the model performance. Fig.2 shows the  
comparison of simulated PNSD with the observations. In Fig.2, the model well  
430 reproduced the evolution of PNSD at the height of 260m at the measurement site. In  
the observation, there are five cycles of conversion from clean days to pollution days.  
Once the pollution episode was over, an obvious new particle formation event  
occurred, such as the events in September 3, 12, 19 and 25. When the pollution level  
increased, the PNSD shifted to end of large diameter. The model well captured the  
435 new particle formation events and the growth of particles in the pollution episode  
mentioned above. Because the atmosphere at higher level was not susceptible to local  
sources, the observation was more representative than that at the ground level. The  
number concentration of particles from 100 nm to 1000 nm was nicely reproduced,  
with normalized bias less than 40% and correlation coefficient being 0.70. The  
440 consistency between simulation and observation suggests the good performance of  
model in producing reasonable number concentration of regional aerosol particles,  
especially in the climate-relevant size range. However, the number concentration of  
particles from 15 nm to 25 nm was overestimated. On one hand, the measurements  
have analytical errors (Du et al., 2017). On the other hand, the model has several  
445 uncertainties. First, the model used the monthly mean emissions and therefore could  
not simulate the diurnal variation of traffic emission. In addition, the size distribution  
of primary emissions does not meet the assumed lognormal distribution. For example,  
traffic sources emit smaller particles than industrial sources (Paasonen et al., 2013;  
Kumar et al., 2014). Second, the nucleation scheme also has uncertainties (Zhang et  
450 al., 2010; Yu et al., 2018). For all this, the main features of new particle formation  
events and the growth of particles were captured by the model. Generally, our model  
produced the aerosols of real atmosphere and the simulation results were reasonable.

The reasonable performance of our model in simulating OA components and  
PNSD gives us the confidence to further analyze the composition of newly formed



455 particles through nucleation and subsequent growth, i.e. SPs in our model. Fig.3a shows the simulated mean contribution of sulfate, nitrate, ammonium, and OA to the mass concentration of SPs in September. Fig.3b shows the contribution of LV anthropogenic OA (LV-AOA), LV biogenic OA (LV-BOA), SV biogenic OA (SV-BOA), and SV anthropogenic OA (SV-AOA) to the mass concentration of OA in  
460 SPs. Fig.3a demonstrate that OA was the major component of SPs, followed by sulfate, nitrate, and ammonium. Among the components of OA in SPs, AOA accounted for 67%, significantly larger than the 33% of BOA, suggesting the dominant role of AOA in particle growth. In terms of volatility, LV-OA took up 67%, in which LV-AOA was responsible for 50% and LV-BOA for 17%. Our model  
465 calculated the gas-phase concentration of LV-SOG and the kinetic condensation of them on size-resolved SPs. The large fraction of LV-AOA in OA of SPs indicates their important role in the growth of SPs. Further, LV-AOA is an indicator of aged atmosphere and its large contribution to OA suggested the influence of regional transport of OA and precursors of OA from surrounding areas to Beijing. The aging  
470 and growth during the lifetime of SPs in the atmosphere could greatly enhance their regional impact. In addition to the local emissions of OA precursors (Guo et al., 2014), our results also highlight the importance of regional sources of OA precursors in the growth of new particles.

## 5.2 Global and regional distribution of OA

475 There are two important characteristics of OA that influence particle growth and particle number concentration: (1) the concentration of OA and (2) the condensation behavior of OA. The concentration of OA is dependent of the OA sources and sinks. The condensation behavior of OA is closely related with the separation of POA and SOA and their volatility distribution. Therefore, these properties of OA are given as  
480 the background to discuss the global and regional particle number concentration. Fig.4 shows the surface distribution of OC concentration and the fraction of secondary OC (SOC) in the Base experiment. In our model, OA is formed by primary emission and the partitioning of gas-phase species onto preexisting organic aerosol. Therefore, the distribution of OC is well correlated with the amount of primary emission and SOA



485 precursors. Globally, the high concentrations of OC are located in the continent  
regions with large emissions. Over China and India, OC concentration can be above  
10  $\mu\text{g}/\text{m}^3$  due to the high emissions from intense anthropogenic activities. In the  
tropical region of Africa, OC concentrations are larger than 5  $\mu\text{g}/\text{m}^3$  due to the  
biomass burning. Over America and Europe, OC concentrations are below 3  $\mu\text{g}/\text{m}^3$ .  
490 The model well reproduced this spatial difference reflected by the observations in  
America and China. The highest concentrations are located in central-eastern China.  
In the second domain (shown in Fig.4c), the highest concentrations of simulated OC  
can be above 15  $\mu\text{g}/\text{m}^3$  over some areas in Sichuan Basin and North China Plain. The  
observed values of OC are underestimated at most sites in China. Firstly, the  
495 difference of time between simulation and observation, especially the emission  
change, could lead to this discrepancy. Secondly, the OA pathways included and the  
parameters used in the model still have uncertainties. Thirdly, the model resolutions  
are not high enough to capture the hot points at cities with small urban areas,  
especially the cities in western China (e.g., Lhasa and Dunhuang). Overall, the model  
500 explained most of the observations. In Fig.4b, it can be seen that SOC dominated most  
regions of the globe with the fraction above 70%. Over China, POC dominated the  
eastern regions while SOC dominated the western regions. In the eastern regions, the  
higher primary emissions lead to the lower fraction of SOC in OC although the SOC  
concentrations are higher than that in western regions.

505 In the VBS in our model, there are three pathways forming SOA, i.e., oxidation  
of POA, oxidation products of anthropogenic and biogenic VOC and IVOC.  
Simulations of most previous studies (Kanakidou et al., 2005; Tsigaridis et al., 2014)  
showed that biogenic SOA (BSOA) is dominant over the global scale due to their  
major sources from the oxidation of biogenic VOCs. However, our simulations shown  
510 in Fig.5 indicate that anthropogenic SOA (ASOA) are as important as the biogenic  
one, especially over the areas with large anthropogenic emissions. Over some areas in  
India and eastern China, concentrations of ASOA can be above 7  $\mu\text{g}/\text{m}^3$ , significantly  
greater than the concentrations of BSOA ( $< 3 \mu\text{g}/\text{m}^3$ ). Even over south America and  
Africa, ASOA has concentrations of 1~3  $\mu\text{g}/\text{m}^3$  due to the large contribution of IVOC



515 and POA emitted from biomass burning. The higher concentrations of ASOA than  
BSOA are also demonstrated by other studies. For example, adding an additional  
SOA correlated with the CO emission can improve the observed OA concentration  
(Spracklen et al. 2011). In the second domain simulation (shown in Fig.5c and 5d), it  
is more clearly seen that ASOA has the higher concentrations than BSOA over China.  
520 In North China Plain, concentrations of ASOA were above  $3 \mu\text{g}/\text{m}^3$  while  
concentrations of BSOA were below  $1 \mu\text{g}/\text{m}^3$ . Previous modeling studies using VBS  
(Han et al., 2016; Lin et al., 2016) also suggested that ASOA is dominant in North  
China. Observation analysis indicated ASOA was the highest one among the  
contributors of SOA sources, very different from the reported cases of developed  
525 countries (Ding et al., 2014; Li et al., 2017; Tang et al., 2018). In addition, our  
simulation considered the SOA formation from IVOC, which has been proved to be a  
large contributor to SOA (Zhao et al., 2016; Yang et al., 2019). Clearly, it is the  
allowing of POA to be volatile and including the SOA formation from IVOC that  
constitute the larger sources of ASOA. The substantial contribution of ASOA to SOA  
530 suggests the significant role of ASOA in particle growth over the areas with intense  
anthropogenic emissions, which will be discussed in Sect.5.4.

Volatility distribution of SOA is a factor controlling not only the mass  
concentrations of OA but also the size distributions of aerosol particles via  
microphysical processes. The framework of VBS can simulate the volatility  
535 distribution of OA in five saturation concentration bins. Study of Riipinen et al. (2011)  
suggested that roughly half of the condensing mass needs to be distributed  
proportional to the aerosol surface area to explain the observed aerosol particle  
growth. The condensation of this part of OA is governed by gas-phase concentration  
rather than the equilibrium vapour pressure, which is the way our model calculates the  
540 growth of LV-SOA to particles. The volatility distribution of SOA is an important  
factor impacting the global and regional distribution of particle number concentration.  
Fig. 6 shows the surface layer spatial distributions of SV-SOA and LV-SOA  
concentrations. Globally, the high concentrations of SV-SOA are mainly located in  
the continental source regions. By contrast, the distribution of LV-SOA is more



545 homogeneous and its contribution to SOA is lower in source regions. The continent  
with higher emission has a lower contribution of LV-SOA. In the downwind regions,  
LV-SOA has the higher concentration than SV-SOA. Even over the source areas, such  
as north America and Europe, LV-SOA also has the higher concentration than  
SV-SOA. These results indicate the multi-generation aging of OA in VBS produce the  
550 higher concentration of LV-SOA and thus the wider spread of OA, which would have  
a large impact on the role of OA in particle formation processes. Over China,  
SV-SOA has the concentration of 3-10  $\mu\text{g}/\text{m}^3$  and is dominant over source areas in  
eastern region. LV-SOA has the concentration of 2-5  $\mu\text{g}/\text{m}^3$  in the eastern region and  
0.6-2  $\mu\text{g}/\text{m}^3$  in the western region. Measurement analysis suggested that OA and SOA  
555 of Beijing in China are more volatile than those of the cities in Europe and America  
(Xu et al., 2019). Our study indicated that, in addition to the different emission  
sources, the more volatile of SOA is also caused by the relative lower contribution of  
LV-SOA to SOA although the concentration of LV-SOA over eastern China is higher  
than that over Europe and America.

### 560 **5.3 Global and regional distribution of particle number concentration**

Fig.7 displays the simulated surface layer horizontal spatial distributions of  
annual mean number concentrations of CN10 and the fraction of CN10 that is  
secondary. The observed CN10 values given in Table 3 are also shown in Fig.6a and  
Fig.7c for comparison. In Fig.7a, it is clear that high concentrations of CN10 in the  
565 surface layer are located in the regions with large anthropogenic emissions. Highest  
concentrations of annual mean CN10 are over the central-eastern China and Sichuan  
basin and their values can be larger than 10000  $\text{cm}^{-3}$ . Over eastern America, most  
areas of European developed countries, and India, values of annual mean CN10 are  
over 5000  $\text{cm}^{-3}$ . Over South America and South Africa, CN10 concentrations are also  
570 higher due to the biomass burning emission. Affected by continental sources and ship  
emissions, CN10 concentrations over the coastal regions and adjacent seas close to the  
continent can be over 1000  $\text{cm}^{-3}$ . Over the polar regions and the oceans far from  
continents, CN10 concentrations are lower than 300  $\text{cm}^{-3}$ . The model well reproduced  
the above spatial variation of CN10 represented by observations in different



575 environments. By a more specific comparison in Fig.8, where the values of simulation  
are compared by a scatter plot with corresponding observations at 34 sites given in  
Table S3, the simulations of annual mean concentration of CN10 agree quite well  
with the observations, within a factor of two for most of the sites. The spatial pattern  
of CN10 over the second domain (in Fig.7c) is similar with that of the corresponding  
580 region in the first domain (in Fig.7a), but the gradients of CN10 is characterized more  
precisely due to the higher horizontal resolution. For example, the high concentrations  
of CN10 over southern Hebei are better depicted in Fig.7c than Fig.7a. The observed  
annual mean CN10 concentration ( $12000 \text{ cm}^{-3}$ ) at Shangdianzi in eastern China was  
five times greater than that of Waliguan ( $2030 \text{ cm}^{-3}$ ) in western China. The  
585 corresponding simulated CN10 concentrations,  $14380 \text{ cm}^{-3}$  and  $2780 \text{ cm}^{-3}$ , well  
reflected this regional difference.

Both secondary particles formed through nucleation and subsequent growth and  
direct emission of primary particles can contribute to atmospheric particle number  
concentration. It is important to quantify the contribution of these two sources in  
590 different parts of the globe. In Fig.6b, it can be seen that secondary particles are  
dominant in most parts of the globe except for the regions with large primary  
emissions, e.g., eastern China, India, and southern Africa. The low contribution of  
secondary particles in these regions is due to the strong scavenging of secondary  
particles by primary particles and the low nucleation rate caused by competing of  
595 primary particles for condensable gases. This spatial pattern is similar with the results  
of previous studies (Yu and Luo, 2009). However, the fractions of secondary particles  
in CN10 are lower than those in CN3 showed in Yu and Luo (2009) due to the  
dominant contribution of secondary nucleation to particles in 3-10 nm. In Fig.7d, a  
boundary from northeast to southwest can be seen to separate the areas dominated by  
600 secondary particles from that by primary particles over China. This phenomenon is  
also caused by the large difference of emissions between western region and eastern  
region.

#### 5.4 The mixing state of organic aerosols and their growth to new particles

Besides particle number concentration, mixing state of aerosols is necessary to



605 evaluate aerosol impacts on climate. The framework of VBS treats the emitted organic  
aerosol with volatility and thus allows them to be partitioned among different aerosol  
particles through condensation. In addition, the evolving volatility due to oxidation in  
the atmosphere makes microphysical behavior of POA to be different from the  
nonvolatile POA. In our model, semi-volatile organics is temperature-driven  
610 partitioned by equilibrium assumption while low-volatility species is kinetically  
condensed on the particles. Fig.9 shows the fraction of organic species reside in  
aerosols of different types (i.e., SPs, sea salt, dust, BC, and OC) defined in our model.  
In Fig.9, most of the organic species reside in OC, SPs, and BC particles, suggesting  
the intense mixing of anthropogenic aerosol species. In the southern hemisphere, the  
615 fractions of organic species residing in SPs are above 30%, larger than that of OC  
particles. In the northern hemisphere, organic species mainly reside in OC particles  
due to the higher concentration of POA and the subsequent partition. The fractions of  
organic species reside in SPs are lower, but still considerable, indicating the important  
role of organic species in forming particles over the whole globe. Due to the different  
620 emission and the associated microphysical processes, there are distinct spatial  
variations of organic species distribution among different continents. Over America,  
30%~40% of OA resides in SPs. By contrast, this fraction is below 20 % over China.  
In China, significant difference also exists between the western and eastern region.  
The dominant contribution of semi-volatile species to OA (shown in Fig.6) and their  
625 partition proportional to the low-volatility OA lead to a higher fraction of organic  
species residing in OC particles over eastern China. The mixing of natural aerosols  
and organic species were also demonstrated in Fig.9. Over the most areas of the globe,  
15% of organic species are distributed in dust particles, which could greatly modify  
the properties of dust particles and thus their climate forcing over the regions  
630 influenced by dust particles (Huang et al., 2019).

Previous study indicate that organic species are the major components of  
aerosols (e.g., Zhang et al., 2007; Jimenez et al., 2009) and low-volatility organic  
species can greatly enhance the growth of new particles (e.g., Yu, 2011; Tröstl et al.,  
2016). Our results presented above also indicated the substantial distribution of



635 organic species in SPs. For this reason, the contribution of LV-SOG to the growth of  
SPs is analyzed. Fig.10 shows the ratio of LV-SOG to  $\text{H}_2\text{SO}_4$  and the ratio of  
low-volatility organic species to sulfate that reside in SPs. The concentration of  
LV-SOG is a factor of  $\sim 1.5$ -10 higher than that of  $\text{H}_2\text{SO}_4$  over many parts of the  
continents and the adjacent oceans but is lower in East Asia, eastern United States,  
640 southern Europe, and northern Africa where emissions of  $\text{SO}_2$  are high. Especially,  
over the areas in Sichuan Basin and eastern China (shown in Fig.10c), the  
concentrations of  $\text{H}_2\text{SO}_4$  are significantly higher than that of LV-SOG. Compared  
with the simulation of Yu (2011), our results included anthropogenic LV-SOG and  
therefore the ratios of LV-SOG to  $\text{H}_2\text{SO}_4$  are higher, especially in the regions  
645 influenced by continental sources and oceans with ship emissions. In Fig.10b and  
Fig.10d, the contribution of low-volatility organic species to the growth of SPs,  
presented by the concentration ratio of low-volatility organic species to sulfate, is  
higher in the southern hemisphere and lower in the northern hemisphere where  
continental sources of  $\text{SO}_2$  are larger. Though lower, the contribution is considerable  
650 ( $\sim 10$ -20%) over Europe and north America. Similar with the contribution of ASOA to  
SOA, LV-SOA residing in SPs is dominated by anthropogenic ones over POA source  
areas (as the case in Beijing shown in Fig.3). The condensation growth of SPs by  
low-volatility organic species can enhance their survival rate and therefore could  
increase the contribution of SPs to particle number concentration. These results  
655 highlight the importance of ASOA in new particle growth over the polluted regions,  
such as eastern China and India.

### 5.5 Sensitivity of particle number concentration to volatility of POA

In the VBS, POA is treated as volatile species and allowed to be aged by  
oxidation in the atmosphere, it is necessary to explore the uncertainties associated  
660 with this treatment of volatility distribution. In addition, the size distribution of POA  
and the associated microphysical processes are also modified due to this treatment.  
For this reason, the sensitivity of particle number concentration to the volatility of  
POA and the assumed size distribution of PPs are discussed here. Fig.11 displays the  
change ratio of number concentrations of CN10 in LV\_POA experiment, HV\_POA



665 experiment, PPD0.5 experiment, and OCD0.5 experiment to that in BASE experiment. Overall, concentration of CN10 changed a little when POA volatilities were in the inter-quartile range of measurements (shown in Fig.11a and b). When using the low/high volatility distribution of POA, PPs number concentrations were increased/decreased by 5-10% over the most areas in the northern hemisphere. By  
670 contrast, SPs number concentrations only had a little change over the areas with the strongest emissions. Due to the dominant contribution of SPs, CN10 had no clear change in most regions of the globe. By contrast, the size distribution of emitted PPs has large influence on the concentration of CN10. When the median diameter of BC and OC use the half size of the BASE experiment, concentrations of CN10 were  
675 increased by 50-150% over the areas with large emission sources of BC and OC, which was too high to matching the observations shown in Fig.7a. For example, the CN10 in PPD0.5 experiment were greatly overestimated when compared with observed concentration ( $12000 \text{ cm}^{-3}$ ) at Shangdianzi in eastern China. Therefore, halving the median diameter of BC and OC in the PPD0.5 experiment could not  
680 represent the real situation. However, halving the median diameter of OC only leads to the increase of CN10 by 10-50% over eastern China. Over the other areas with high emission, there was no observation available for comparison. Considering the other factors affecting the simulation of CN10, it is not safe to say that the assumed median size of OC is too small in the PPD0.5 experiment. Moreover, the emitted OC particles  
685 indeed have volatility and can re-evaporation after dilution (Robinson et al., 2007; Donahue et al., 2009). The assumption of OC size distribution should take volatility of OC into account. It is necessary to measure the size distribution of freshly emitted primary particles and compare the model results with observation in polluted atmosphere dominated by PPs to clarify this issue.

## 690 **6 Conclusion and discussion**

The sources of organic aerosol, volatility distribution, and the microphysical behavior of organic species have been found to be important in particle formation processes by laboratory studies and field observations, but the organic aerosol processes are still poorly represented and they are the large contributors to model



695 uncertainties in simulating aerosol microphysical properties. In this study, a new  
global-regional nested aerosol model was developed to simulate detailed  
microphysical processes in the real atmosphere. The new model combined APM  
module and VBS module to simulate microphysical processes of OA. In the model,  
the OA in the lowest volatility bin is treated as non-volatile/low-volatile species and  
700 their condensation was simulated by the kinetic way. The OA in other volatility bins  
was simulated by equilibrium partitioning. Using this framework, both the  
condensation of secondary inorganic species (i.e., sulfuric acid, nitrate, and  
ammonium) and the condensation of organic species with different volatilities (i.e.,  
low-volatility and semi-volatile organic compounds) were simultaneously simulated,  
705 which is an important advances of our new model. The concentration of low-volatility  
organics is separately calculated and the condensation of  $\text{H}_2\text{SO}_4$  and LV-SOG on  
size-resolved secondary particles is explicitly simulated, along with the condensation  
of LV-SOG on primary particles. Therefore, the growth of LV-SOG to new particles  
and aging of primary particles by organic species were represented in a realistic way.  
710 Compared with the most models in the second phase AeroCom (Tsigaridis et al., 2014;  
Mann et al., 2014) and the recently developed new models (e.g., Yu, 2011; Patoulias  
et al., 2015; Gao et al., 2017), our model includes the more comprehensive sources of  
SOA by using the VBS framework, especially the anthropogenic SOA. In addition,  
allowing POA to evaporate and re-condense onto the particles make its microphysical  
715 behavior more like SOA and therefore give new meaning to the POA–SOA split  
which significantly affects the global CCN formation (Trivitayanurak and Adams,  
2014). The flexible framework of APM combined with VBS produces the different  
distribution of organic species in aerosols, i.e., the mixing state of OA, which has  
been found to cause substantial difference in radiative effects of aerosols (Zhu et al.,  
720 2017). Box model analyses showed that the low-volatility SOA has a large fraction in  
the growing nucleation mode particles (Pierce et al., 2011). The comprehensive  
thermodynamic-kinetic approach treating the condensation and the partitioning of  
organic species originated from biogenic and anthropogenic sources allows us to  
investigate the full role of organic species in the growth of new particles, which is



725 important for understanding the formation processes of particles relevant for radiative forcing and clouds (Shrivastava et al., 2017).

The model with three nested domains was applied to simulate the aerosol components and PNSD in Megacity Beijing during a period of about a month. The simulation results were evaluated by the observations at the high level of IAP tower, which is more representative than the ground level in regional scale. The simulated BC and OA components agreed well with the PMF analysis of AMS measurements. The evolution of PNSD and NPF events were also nicely reproduced by the model. Our modeling analyses showed that AOA accounts for the larger part of OA of SPs and thus significantly contributed to the growth of SPs in Beijing. Molteni et al. (2018) indicated highly oxygenated organic compounds formed from anthropogenic VOCs can substantially contribute to NPF in urban areas. Observations in Beijing suggested that anthropogenic VOCs are major constituents of SOA (Ding et al., 2015; Yang et al., 2016). For the first time, the contribution of AOA to new particles was quantified benefiting from the mixing state our model resolved in our study. Although the exact role of AOA in NPF is not quite clear, our study explicitly displayed the important role of AOA in NPF in Chinese megacities, which would help elucidate the mechanism of more frequent occurrences of NPF events than theoretical prediction in polluted atmosphere (Kulmala et al., 2017; Chu et al., 2019). By comparison with the observations collected from published data, the model well reproduced the annual mean concentration of the observed OC at continent sites in America and China. Due to the re-evaporation and oxidation of POA and the additional emission of IVOC, ASOA becomes dominant in SOA over POA source areas. At sites in different environments over the globe, the model produced the reasonable concentrations of CN10 within a factor of two for most of the sites. LV-SOG, especially the anthropogenic SOA, was found to have a large contribution to new particle growth over areas with intense anthropogenic emissions, such as in eastern China. The global simulation of Kelly et al. (2018) found that including the large anthropogenic SOA source could get results consistent with observations over the northern hemisphere mid-latitudes. Simulation over East Asia also indicated that most of the OA were from



755 anthropogenic sources (Matsui et al., 2014). Together with these studies, our modeling  
results further provided the direct evidence of AOA in particle formation processes  
not only in Chinese megacities but also in other regions influenced by anthropogenic  
sources in the global scale.

Sensitivity analyses indicate that concentration of CN10 only changed a little in  
760 the regions with the highest emission of POA and had no clear change in most regions  
of the globe when POA volatilities were in the inter-quartile range of measurements.  
Although the size distribution of primary emitted particles has large impact on the  
simulation of CN10 as suggested by other studies (e.g., Spracklen et al., 2006; Chang  
et al., 2009; Zhou et al., 2018), the simulation of the base experiment gave the better  
765 agreement with the observations than the sensitivity experiments and the conclusions  
will not be changed. Even so, the importance of the size distribution of primary  
emitted particles should be emphasized. The global model results have suggested the  
high sensitivity of CCN to to the assumed emission size distribution (Lee et al., 2013).  
Recently, Xausa et al. (2018) found that using the size-segregated primary particle  
770 number emissions could make the number concentration of accumulation mode  
particles closer to the measurements. Here, our simulation indicates to the importance  
of parameterization of the size distribution of emitted OC particles after considering  
their re-evaporation and condensation. Therefore, it is necessary to constrain the  
primary emission both in their size distribution and volatility. In addition, it should be  
775 noted that the simulated properties of OA were also determined by the parameters of  
VBS module, the emissions inventory and meteorological fields input to the model,  
and the physicochemical processes in the model. Although our model gave the  
reasonable calculation comparable with the available observations and model results  
of other authors, it is still necessary to further improve our model in the future. For  
780 example, the size-resolved emissions of anthropogenic primary particles will be used  
as the model input to reducing the uncertainties associated. More nucleation schemes  
will be implemented into the model to investigate the influence of nucleation schemes  
on the aerosol number concentrations as the uncertainties from nucleation scheme are  
still large (Dunne et al., 2016). Aqueous-phase formation processes of SOA have



785 evident influence on the particle properties and total SOA mass (Ervens et al., 2011)  
and these processes can close the gap between the simulation and observation (Lin et  
al., 2014). It is necessary to refine the description of aerosol microphysical processes  
by including aqueous formation of SOA in our model.

790

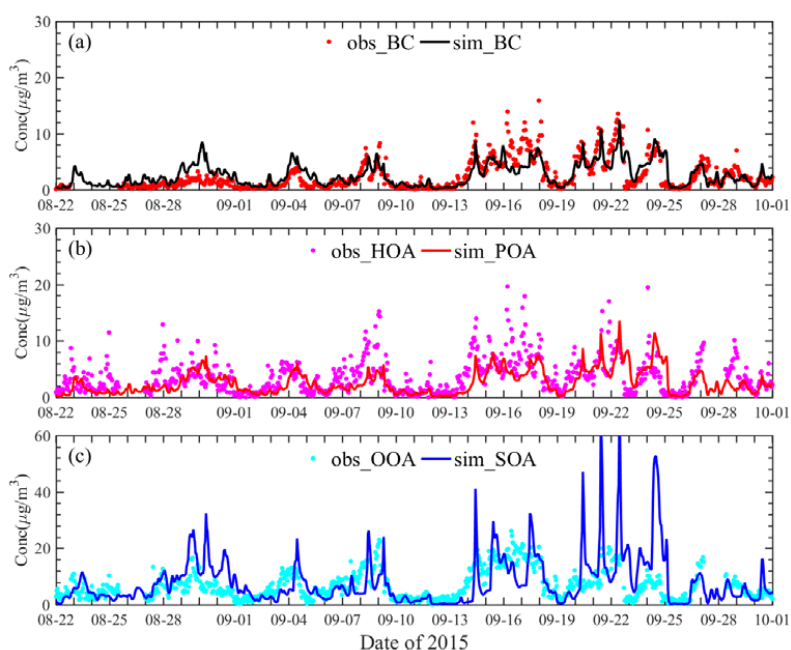


Fig.1 Comparison of the simulated and the observed (a) black carbon, (b) primary organic aerosol,  
and (c) secondary organic aerosol at the 260m height in Beijing from August 22 to September 30,  
2015. All the observations were shown with dot points and the simulations with lines.

795

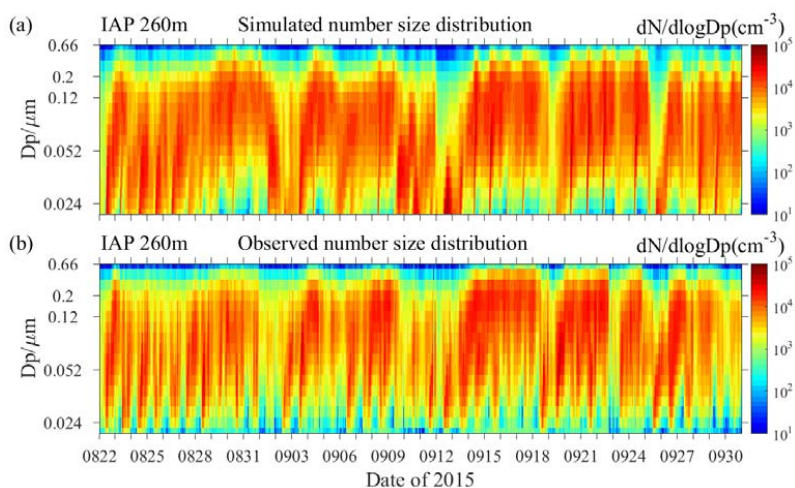
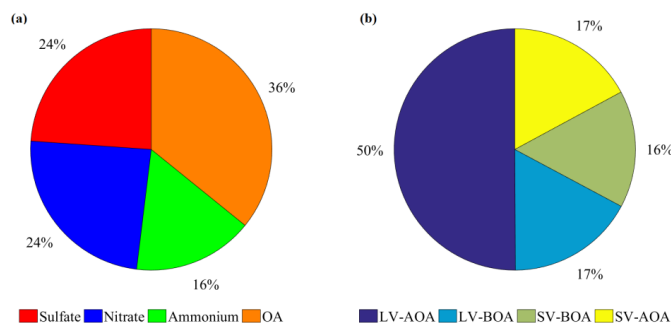
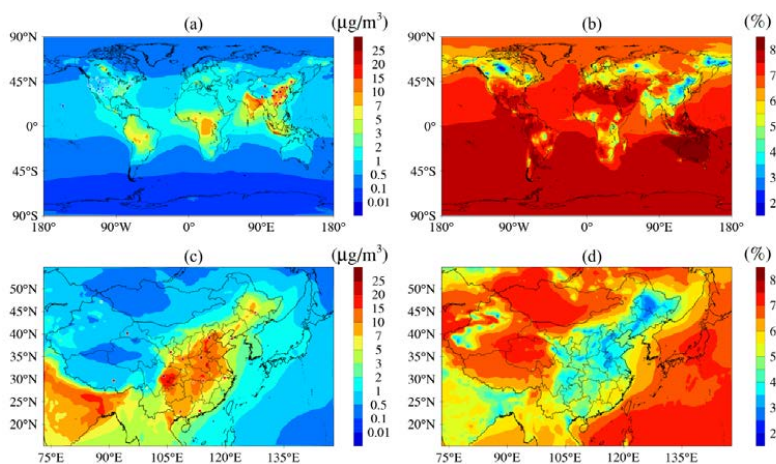


Fig.2 (a) Simulated and (b) observed particle number size distribution at high level (260 m) in Beijing from August 22 to September 30, 2015.



800

Fig.3 (a) The mean contribution of sulfate, nitrate, ammonium, and OA to the mass concentration of SPs and (b) the mean contribution of LV-AOA, LV-BOA, SV-BOA, and SV-AOA to the mass concentration of OA in SPs in September, 2015.



805

Fig. 4. Surface layer horizontal spatial distributions of organic carbon concentrations (left panel) and the fraction of OC that is secondary (right panel) over the first domain (top panel) and second domain (bottom panel). Observed OC collected in Sect.4 are also overlapped with shaded circles on the plots for comparison.

810

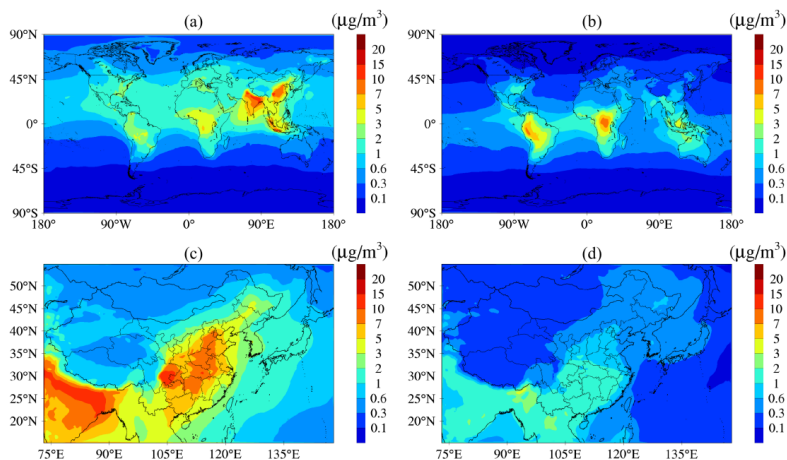


Fig. 5. Surface layer horizontal spatial distributions of ASOA concentrations (left panel) and BSOA concentrations (right panel) over the first domain (top panel) and second domain (bottom panel).

815

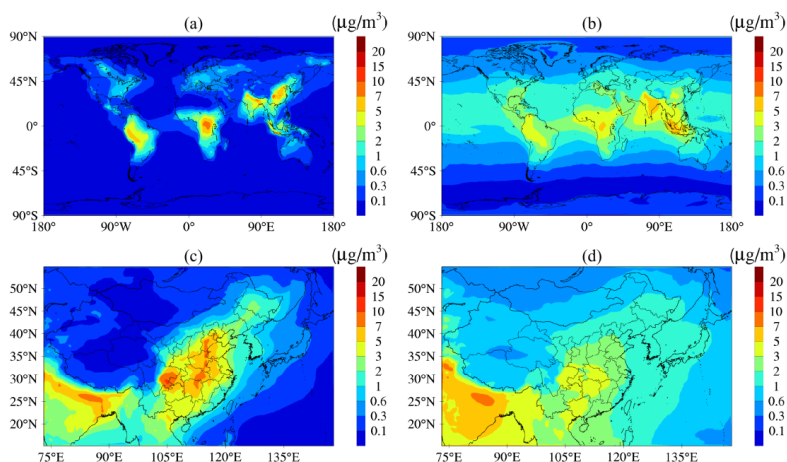


Fig. 6. Surface layer horizontal spatial distributions of SV-SOA concentrations (left panel) and LV-SOA concentrations (right panel) over the first domain (top panel) and second domain (bottom panel).

820

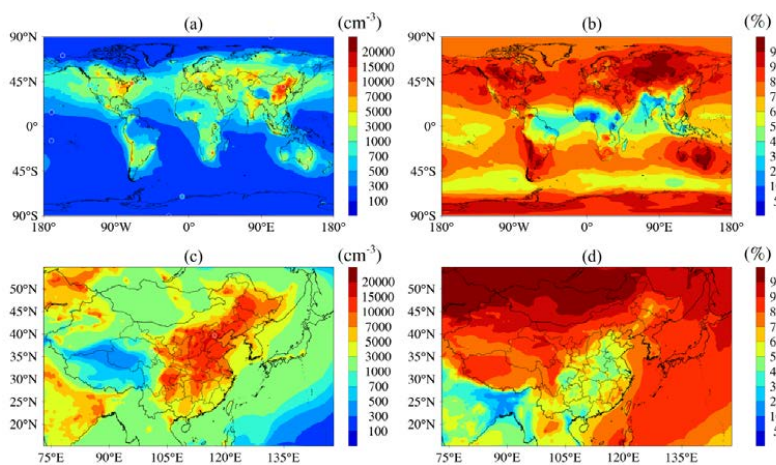
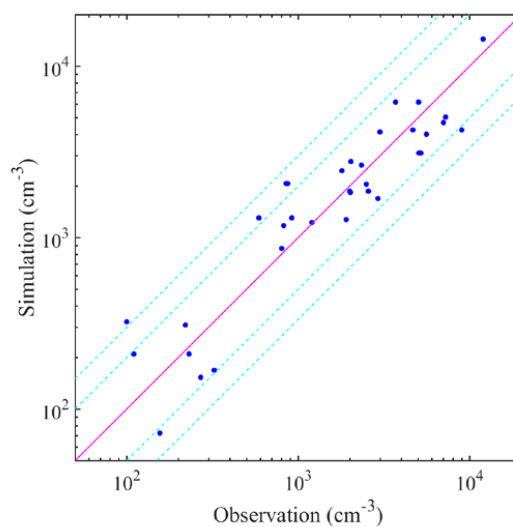


Fig. 7. Surface layer horizontal spatial distributions of annual mean number concentrations of CN10 (left panel) and fraction of CN10 that is secondary (right panel) over the first domain (top panel) and second domain (bottom panel). Observed CN10 values in Table 3 are also overlapped

825

with shaded circles on the plots for comparison.



830 Fig. 8. Comparison of simulated and observed annual mean number concentrations of particles condensation larger than 10 nm at 34 sites listed in Table 3. The solid carmine line shows a 1:1 ratio and the dashed turquoise lines show ratios of 3:1, 2:1, 1:2, and 1:3.

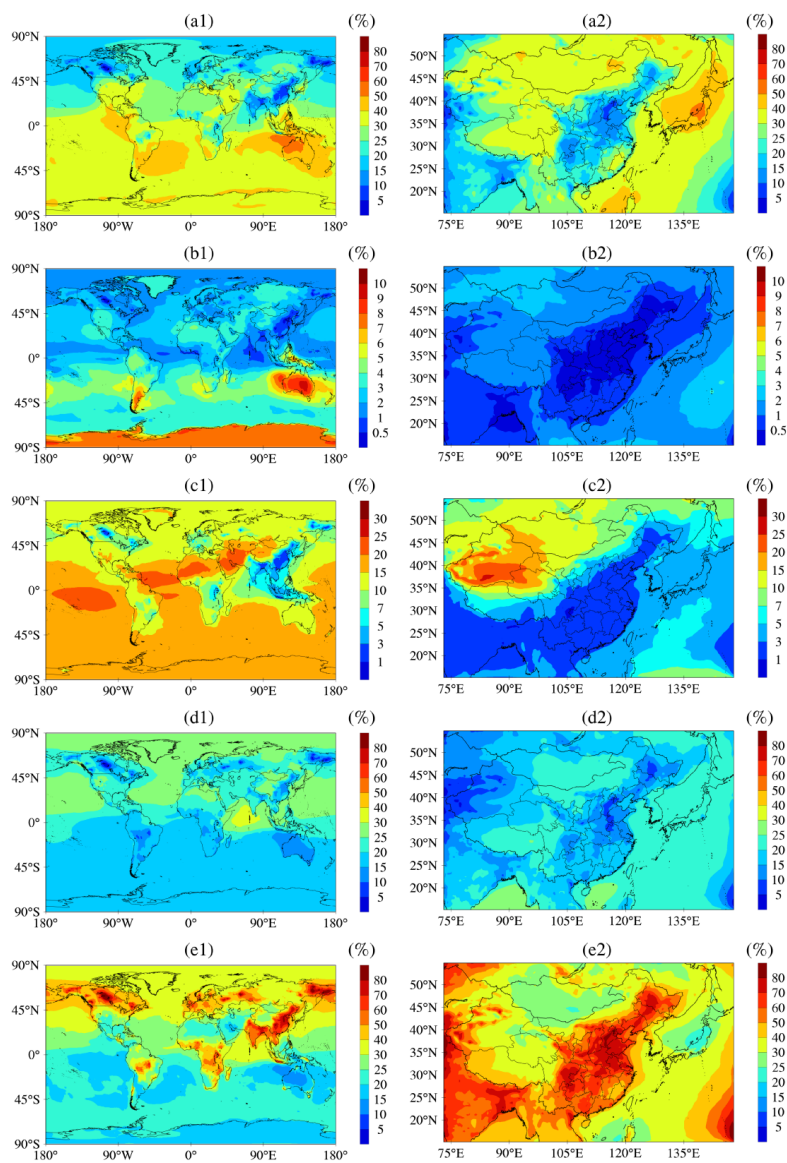


Fig. 9. Surface layer horizontal spatial distributions of the fraction of organic species that reside in SP (a1 and a2), sea salt (b1 and b2), dust (c1 and c2), BC (d1 and d2), and OC (e1 and e2) particles over the first domain (top panel) and second domain (bottom panel).

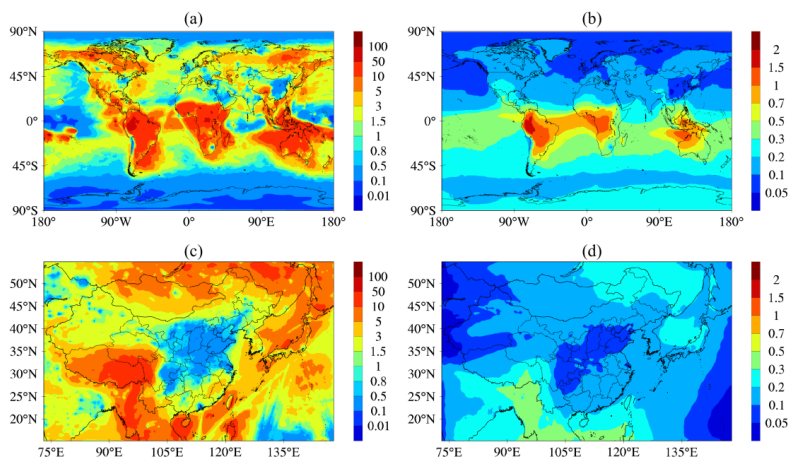


Fig. 10. The ratio of LV-SOG to  $\text{H}_2\text{SO}_4$  (left panel) and the ratio of LV-OA to sulfate (right panel) that reside in SPs. Top panel is for the first domain and bottom panel for the second domain.

840

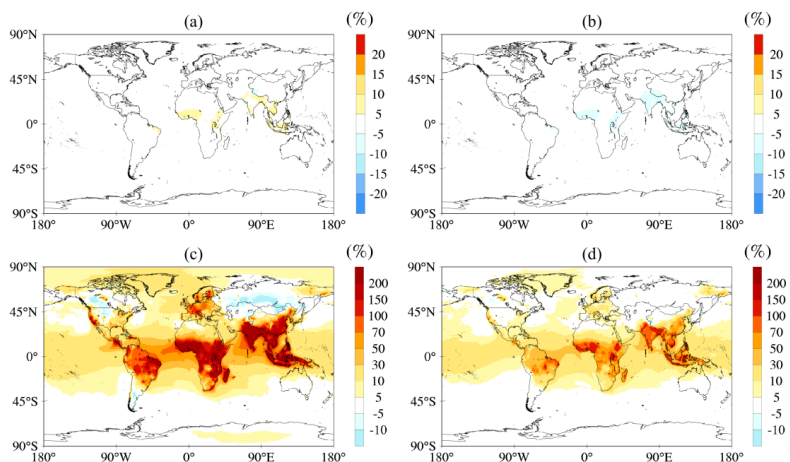


Fig. 11. Relative change of number concentrations of CN10 in (a) LV\_POA experiment, (b) HV\_POA experiment, (c) PPD0.5 experiment, and (d) OCD0.5 experiment to that in BASE experiment.

845

Table 1 The newly added tracers for simulation in microphysical processes

Tracers	Description
$\text{H}_2\text{SO}_4$	Sulfuric acid gas
LV-SOG	Low-volatility secondary organic gas



Sulfate(1-40)	Size-resolved sulfate of secondary particles in 40 bins
BC(1-28)	Size-resolved black carbon in 28 bins
POC(1-28)	Size-resolved primary organic carbon in 28 bins
Sea salt(1-20)	Size-resolved sea salt in 20 bins
Dust(1-4)	Size-resolved dust in 4 bins
BC_Sulfate	Sulfate coated on BC
OC_Sulfate	Sulfate coated on OC
Sea salt_Sulfate	Sulfate coated on sea salt
Dust_Sulfate	Sulfate coated on dust
SP-LV	Low-volatility organic aerosol coated on SPs
Salt-LV	Low-volatility organic aerosol coated on sea salt
Dust-LV	Low-volatility organic aerosol coated on dust
BC-LV	Low-volatility organic aerosol coated on BC
OC-LV	Low-volatility organic aerosol coated on POC

850 Table 2 Sensitivity experiments and their description. The “Primary size” column refers to the geometric mean diameter values (nm) assumed for primary carbonaceous aerosol emissions. The “Volatility distribution” column refers to the coefficients of POA distributed to the volatility bins for vehicles, other anthropogenic, biomass burning, respectively. Coefficients for different sources are separated by semicolons, and different bins (from the lowest to the highest) by commas.

Experiments	Primary size	Volatility distribution
BASE	60, 150 (1.80, 1.80) for BC and POC	0.27, 0.15, 0.26, 0.15, 0.17; 0.167, 0.167, 0.243, 0.197, 0.226; 0.2, 0.1, 0.1, 0.2, 0.4
LV_POA	60, 150 (1.80, 1.80) for BC and POC	0.34, 0.21, 0.3, 0.1, 0.05; 0.234, 0.217, 0.27, 0.157, 0.122 ; 0.25, 0.15, 0.15, 0.2, 0.25
HV_POA	60, 150 (1.80, 1.80) for BC and POC	0.16, 0.21, 0.21, 0.19, 0.33; 0.11, 0.093, 0.217, 0.217, 0.363 ; 0.15, 0.05, 0.05, 0.2, 0.55
OCD0.5	30,75 (1.80, 1.80) for POC	0.27, 0.15, 0.26, 0.15, 0.17; 0.167, 0.167, 0.243, 0.197, 0.226; 0.2, 0.1, 0.1, 0.2, 0.4



PPD0.5	30,75 (1.80, 1.80) for	0.27, 0.15, 0.26, 0.15, 0.17; 0.167, 0.167, 0.243,
	BC and POC	0.197, 0.226; 0.2, 0.1, 0.1, 0.2, 0.4

---

855 **Data availability.** All of the observation in this paper are provided in the manuscript.  
The simulation data can be available from the authors upon request  
(chenxsh@mail.iap.ac.cn, zifawang@mail.iap.ac.cn).

**Author contribution.** XC developed the model, performed the simulations and  
860 analysis, and prepared the manuscript with contributions from all co-authors. FY  
provided the code of APM module and modified the manuscript. WY coupled the  
VBS module and modified the manuscript. YS, WD, and JZ provided the observation  
data at Beijing site and modified the manuscript. HC prepared the emission data and  
modified the model code. YW, LW, HD, ZW, QW, JL, and JA modified the  
865 manuscript. ZW guided the study and modified the manuscript.

**Competing interests.** The authors declare that they have no conflict of interest.

**Acknowledgement.** This work was supported by the National Key R&D Program of  
870 China (Grant No. 2017YFC0209801 and Grant No. 2017YFC0209805) and the  
National Natural Science Foundation of China (Grant No. 41705108, 41907200, and  
41907201).

## References

- 875 Ahmadov, R., McKeen, S., Robinson, A., Bahreini, R., Middlebrook, A., de Gouw, J., Meagher, J.,  
Hsie, E. Y., Edgerton, E., Shaw, S., and Trainer, M.: A volatility basis set model for  
summertime secondary organic aerosols over the eastern United States in 2006, *Journal of  
Geophysical Research (Atmospheres)*, 117, 6301, 10.1029/2011JD016831, 2012.
- 880 Albrecht, B.: Aerosols, Cloud Microphysics, and Fractional Cloudiness, *Science (New York,  
N.Y.)*, 245, 1227-1230, 10.1126/science.245.4923.1227, 1989.



- Athanasopoulou, E., Tombrou, M., Pandis, S., and Russell, A.: The role of sea-salt emissions and heterogenous chemistry in the air quality of polluted coastal areas, *Atmospheric Chemistry and Physics*, 8, 10.5194/acpd-8-3807-2008, 2008.
- 885 Bergman, T., Kerminen, V.-M., Korhonen, H., Lehtinen, K., Makkonen, R., Arola, A., Mielonen, T., Romakkaniemi, S., Kulmala, M., and Kokkola, H.: Evaluation of the sectional aerosol microphysics module SALSIA implementation in ECHAM5-HAM aerosol-climate model, *Geoscientific Model Development Discussions*, 4, 3623-3690, 10.5194/gmdd-4-3623-2011, 2011.
- 890 Binkowski, F., and Shankar, U.: The Regional Particulate Matter Model. 1. Model description and preliminary results, *Journal of Geophysical Research*, 1002, 26191-26210, 10.1029/95JD02093, 1995.
- Boy, M., Kulmala, M., Ruuskanen, T. M., Pihlatie, M., Reissell, A., Aalto, P. P., Keronen, P., Dal Maso, M., Hellen, H., Hakola, H., Jansson, R., Hanke, M., and Arnold, F.: Sulphuric acid closure and contribution to nucleation mode particle growth, *Atmos. Chem. Phys.*, 5, 863-878, 10.5194/acp-5-863-2005, 2005.
- 895 Byun, D., and Dennis, R.: Design artifacts in eulerian air quality models: Evaluation of the effects of layer thickness and vertical profile correction on surface ozone concentrations, *Atmospheric Environment*, 29, 105-126, 10.1016/1352-2310(94)00225-A, 1995.
- 900 C, K., Riipinen, I., Sihto, S.-L., Kulmala, M., McCormick, A., and McMurry, P.: An improved criterion for new particle formation in diverse atmospheric environments, *Atmospheric Chemistry and Physics*, 10, 10.5194/acp-10-8469-2010, 2010.
- C, T., Michael, S., S, G., S, K., Balkanski, Y., S, B., Berntsen, T., Berglen, T., Boucher, O., Chin, M., Dentener, F., Diehl, T., Easter, R., H, F., D, F., Ghan, S., Ginoux, P., Gong, S., A, G., and Tie, X.: Analysis and quantification of the diversities of aerosol life cycles within AeroCom, *Atmospheric Chemistry and Physics*, 6, 10.5194/acp-6-1777-2006, 2006.
- 905 Chang, L.-S., Schwartz, S., McGraw, R., and Lewis, E.: Sensitivity of aerosol properties to new particle formation mechanism and to primary emissions in a continental-scale chemical transport model, *J. Geophys. Res.*, 114, 10.1029/2008JD011019, 2009.
- 910 Charlson, R., Schwartz, S., Hales, J., Cess, R., Coakley, Jr., Hansen, J., and Hofmann, D.: Climate Forcing by Anthropogenic Aerosols, *Science (New York, N.Y.)*, 255, 423-430, 10.1126/science.255.5043.423, 1992.
- Chen, H., Wang, Z., Li, J., Tang, X., ge, B., Wu, X., Wild, O., and Carmichael, G.: GNAQPMS-Hg v1.0, a global nested atmospheric mercury transport model: model description, evaluation and application to trans-boundary transport of Chinese anthropogenic emissions, *Geoscientific Model Development*, 8, 10.5194/gmd-8-2857-2015, 2015.
- 915 Chen, X.: Simulation on microphysics of fine particles over central-eastern China. (Doctoral dissertation, University of Chinese Academy of Sciences), 2015.
- 920 Chen, X., Wang, Z., Li, J., and Yu, F.: Development of a Regional Chemical Transport Model with Size-Resolved Aerosol Microphysics and Its Application on Aerosol Number Concentration Simulation over China, *SOLA*, 10, 83-87, 10.2151/sola.2014-017, 2014.
- Chen, X., Wang, Z., Li, J., Chen, H., Hu, M., Yang, W., Wang, Z., ge, B., and Wang, D.: Explaining the spatiotemporal variation of fine particle number concentrations over Beijing



- and surrounding areas in an air quality model with aerosol microphysics, *Environmental pollution*, 231, 10.1016/j.envpol.2017.08.103, 2017.
- 925 Chen, X., Wang, Z., Li, J., Yang, W., Chen, H., Wang, Z., Hao, J., ge, B., Wang, D., and Huang, H.: Simulation on different response characteristics of aerosol particle number concentration and mass concentration to emission changes over mainland China, *The Science of the total environment*, 643, 692-703, 10.1016/j.scitotenv.2018.06.181, 2018.
- 930 Chen, X., Yang, W., Wang, Z., Li, J., Hu, M., An, J., Wu, Q., Wang, Z., Chen, H., Wei, Y., Du, H., and Wang, D.: Improving new particle formation simulation by coupling a volatility-basis set (VBS) organic aerosol module in NAQPMS+APM, *Atmospheric Environment*, 204, 1-11, 10.1016/j.atmosenv.2019.01.053, 2019.
- 935 Chu, B., Kerminen, V.-M., Bianchi, F., Yan, C., Petäjä, T., and Kulmala, M.: Atmospheric new particle formation in China, *Atmospheric Chemistry and Physics*, 19, 115-138, 10.5194/acp-19-115-2019, 2019.
- D'Andrea, S., Häkkinen, S., Westervelt, D., Kuang, C., Levin, E., Kanawade, V., Leaitch, W., Spracklen, D., Riipinen, I., and Pierce, J.: Understanding global secondary organic aerosol amount and size-resolved condensational behavior, *Atmos. Chem. Phys.*, 13, 11519-11534, 10.5194/acp-13-11519-2013, 2013.
- 940 Delfino, R., Sioutas, C., and Malik, S.: Potential Role of Ultrafine Particles in Associations between Airborne Particle Mass and Cardiovascular Health, *Environmental health perspectives*, 113, 934-946, 10.1289/ehp.7938, 2005.
- Ding, X., He, Q.-F., Shen, R.-Q., Yu, Q.-Q., and Wang, X.-M.: Spatial distributions of secondary organic aerosols from isoprene, monoterpenes,  $\beta$ -caryophyllene, and aromatics over China during summer, 119, 11,877-811,891, 10.1002/2014jd021748, 2014.
- 945 Donahue, N., Robinson, A. L., Stanier, C., and Pandis, S.: Coupled Partitioning, Dilution, and Chemical Aging of Semivolatile Organics, *Environmental science & technology*, 40, 2635-2643, 10.1021/es052297c, 2006.
- 950 Donahue, N., Robinson, A., and Pandis, S.: Atmospheric organic particulate matter: From smoke to secondary organic aerosol, *Atmospheric Environment*, 43, 94-106, 10.1016/j.atmosenv.2008.09.055, 2009.
- Donahue, N., Trump, E., Pierce, J., and Riipinen, I.: Theoretical constraints on pure vapor-pressure driven condensation of organics to ultrafine particles, *Geophysical Research Letters - GEOPHYS RES LETT*, 38, 10.1029/2011GL048115, 2011.
- 955 Donahue, N., Kroll, J., Pandis, S., and Robinson, A.: A two-dimensional volatility basis set – Part 2: Diagnostics of organic-aerosol evolution, *Atmospheric Chemistry and Physics*, 12, 10.5194/acp-12-615-2012, 2012.
- 960 Donahue, N., Chuang, W., Epstein, S., Kroll, J., Worsnop, D., Robinson, A., Adams, P., and Pandis, S.: Why do organic aerosols exist? Understanding aerosol lifetimes using the two-dimensional volatility basis set, *Environmental Chemistry*, 10, 151, 10.1071/EN13022, 2013.
- 965 Donaldson, K., Brown, D., Clouter, A., Duffin, R., MacNee, W., Renwick, L., Tran, L., and Stone, V.: The Pulmonary Toxicology of Ultrafine Particles, *Journal of aerosol medicine : the official journal of the International Society for Aerosols in Medicine*, 15, 213-220, 10.1089/089426802320282338, 2002.



- Du, H., Li, J., Chen, X., Wang, Z., Sun, Y., Fu, P., Li, J., Gao, J., and Wei, Y.: Modeling of aerosol property evolution during winter haze episodes over a megacity cluster in northern China: roles of regional transport and heterogeneous reactions of SO<sub>2</sub>, *Atmos. Chem. Phys.*, 19, 9351-9370, 10.5194/acp-19-9351-2019, 2019.
- 970 Du, W., Zhao, J., Yuying, W., Zhang, Y., Wang, Q., Xu, W., Chen, C., Han, T., Zhang, F., Li, z., Fu, P., Li, J., Wang, Z., and Sun, Y.: Simultaneous measurements of particle number size distributions at ground level and 260 m on a meteorological tower in urban Beijing, China, *Atmospheric Chemistry and Physics*, 17, 6797-6811, 10.5194/acp-17-6797-2017, 2017.
- Dunne, E. M., Gordon, H., Kurten, A., Almeida, J., Duplissy, J., Williamson, C., Ortega, I. K., Pringle, K. J., Adamov, A., Baltensperger, U., Barmet, P., Benduhn, F., Bianchi, F., Breitenlechner, M., Clarke, A., Curtius, J., Dommen, J., Donahue, N. M., Ehrhart, S., Flagan, R. C., Franchin, A., Guida, R., Hakala, J., Hansel, A., Heinritzi, M., Jokinen, T., Kangasluoma, J., Kirkby, J., Kulmala, M., Kupc, A., Lawler, M. J., Lehtipalo, K., Makhmutov, V., Mann, G., Mathot, S., Merikanto, J., Miettinen, P., Nenes, A., Onnela, A., 980 Rap, A., Reddington, C. L., Riccobono, F., Richards, N. A., Rissanen, M. P., Rondo, L., Sarnela, N., Schobesberger, S., Sengupta, K., Simon, M., Sipila, M., Smith, J. N., Stozkhov, Y., Tome, A., Trostl, J., Wagner, P. E., Wimmer, D., Winkler, P. M., Worsnop, D. R., and Carslaw, K. S.: Global atmospheric particle formation from CERN CLOUD measurements, *Science*, 354, 1119-1124, 10.1126/science.aaf2649, 2016.
- 985 Ervens, B., Turpin, B. J., and Weber, R. J.: Secondary organic aerosol formation in cloud droplets and aqueous particles (aqSOA): a review of laboratory, field and model studies, *Atmos. Chem. Phys.*, 11, 11069–11102, <https://doi.org/10.5194/acp-11-11069-2011>, 2011.
- Ervens, B., Sorooshian, A., Lim, Y., and Turpin, B.: Key parameters controlling OH-initiated formation of secondary organic aerosol in the aqueous phase (aqSOA), *Journal of Geophysical Research: Atmospheres*, 119, 10.1002/2013JD021021, 2014.
- 990 Farina, S., Adams, P., and Pandis, S.: Modeling global secondary organic aerosol formation and processing with the volatility basis set: Implications for anthropogenic secondary organic aerosol, *Journal of Geophysical Research*, 115, 10.1029/2009JD013046, 2010.
- Fountoukis, C., Racherla, P., Denier van der Gon, H., Polymeneas, P., Haralabidis, P., Wiedensohler, A., Pilinis, C., and Pandis, S.: Evaluation of a three-dimensional chemical transport model (PMCAMx) in the European domain during the EUCAARI May 2008 campaign, *Atmospheric Chemistry and Physics Discussions*, 11, 14183-14220, 10.5194/acpd-11-14183-2011, 2011.
- 995 Fu, T.-M., Cao, J., Zhang, X., Lee, S., Zhang, Q., Han, Y., Qu, W., Han, Z., Zhang, R., Wang, Y., Chen, D., and Henze, D.: Carbonaceous aerosols in China: Top-down constraints on primary sources and estimation of secondary contribution, in, 2014.
- 1000 Gao, C., Tsigaridis, K., and Bauer, S.: MATRIX-VBS (v1.0): Implementing an evolving organic aerosol volatility in an aerosol microphysics model, *Geoscientific Model Development*, 10, 751-764, 10.5194/gmd-10-751-2017, 2017.
- 1005 Gkatzelis, G. I., Papanastasiou, D. K., Florou, K., Kaltsonoudis, C., Louvaris, E., and Pandis, S. N.: Measurement of nonvolatile particle number size distribution, *Atmos. Meas. Tech.*, 9, 103-114, 10.5194/amt-9-103-2016, 2016.
- Goldstein, A., and Galbally, I.: Known and Unexplored Organic Constituents in the Earth's Atmosphere, *Environmental Science and Technology*, 41, 10.1021/es072476p, 2007.



- 1010 Guo, S., Hu, M., Levy Zamora, M., Peng, J., Shang, D., Du, Z., Wu, Z., Shao, M., Zeng, L., Molina, M., and Zhang, R.: Elucidating severe urban haze formation in China, *Proceedings of the National Academy of Sciences of the United States of America*, 111, 10.1073/pnas.1419604111, 2014.
- 1015 Guo, S., Hu, M., Peng, J., Wu, Z., Levy Zamora, M., Shang, D., Du, Z., Xin, F., Tang, R., Wu, Y., Zeng, L., Shuai, S., Zhang, W., Wang, Y., Ji, Y.-M., Li, Y., Zhang, A., Wang, W., and Zhang, R.: Remarkable nucleation and growth of ultrafine particles from vehicular exhaust, *Proceedings of the National Academy of Sciences*, 117, 201916366, 10.1073/pnas.1916366117, 2020.
- 1020 Hallquist, M., Wenger, J. C., Baltensperger, U., Rudich, Y., Simpson, D., Claeys, M., Dommen, J., Donahue, N. M., George, C., Goldstein, A. H., Hamilton, J. F., Herrmann, H., Hoffmann, T., Iinuma, Y., Jang, M., Jenkin, M. E., Jimenez, J. L., Kiendler-Scharr, A., Maenhaut, W., McFiggans, G., Mentel, T. F., Monod, A., Prévôt, A. S. H., Seinfeld, J. H., Surratt, J. D., Szmigielski, R., and Wildt, J.: The formation, properties and impact of secondary organic aerosol: current and emerging issues, *Atmos. Chem. Phys.*, 9, 5155-5236, 10.5194/acp-9-5155-2009, 2009.
- 1025 Han, S.: Effect of Aerosols on Visibility and Radiation in Spring 2009 in Tianjin, China, *Aerosol and Air Quality Research*, 10.4209/aaqr.2011.05.0073, 2012.
- 1030 Han, Z., Xie, Z., Wang, G., Zhang, R., and Tao, J.: Modeling organic aerosols over east China using a volatility basis-set approach with aging mechanism in a regional air quality model, *Atmospheric Environment*, 124, 10.1016/j.atmosenv.2015.05.045, 2015.
- Han, Z., Xie, Z., Wang, G., Zhang, R., and Tao, J.: Modeling organic aerosols over east China using a volatility basis-set approach with aging mechanism in a regional air quality model, *Atmospheric Environment*, 124, 186-198, <https://doi.org/10.1016/j.atmosenv.2015.05.045>, 2016.
- 1035 Harrison, R., and Jones, A.: Multisite Study of Particle Number Concentrations in Urban Air, *Environmental science & technology*, 39, 6063-6070, 10.1021/es040541e, 2005.
- 1040 Hodzic, A., Kasibhatla, P. S., Jo, D. S., Cappa, C. D., Jimenez, J. L., Madronich, S., and Park, R. J.: Rethinking the global secondary organic aerosol (SOA) budget: stronger production, faster removal, shorter lifetime, *Atmos. Chem. Phys.*, 16, 7917-7941, 10.5194/acp-16-7917-2016, 2016.
- Holmes, N. S.: A review of particle formation events and growth in the atmosphere in the various environments and discussion of mechanistic implications, *Atmospheric Environment*, 41, 2183-2201, <https://doi.org/10.1016/j.atmosenv.2006.10.058>, 2007.
- 1045 Huang, J., Ma, J., Guan, X., Li, Y., and He, Y.: Progress in Semi-arid Climate Change Studies in China, *Advances in Atmospheric Sciences*, 36, 922-937, 10.1007/s00376-018-8200-9, 2019.
- IPCC (Intergovernmental Panel on Climate Change): *ClimateChange 2013: The Physical Science Basis. Contribution of Working Group I to the Fifth Assessment, Report of the Intergovernmental Panel on Climate Change*, Cambridge University Press, Cambridge, United Kingdom, and New York, NY, USA.
- 1050 Jacobson, M., Turco, R., Jensen, E., and Toon, O.: Modeling Coagulation Among Particles of Different Composition and Size, *Atmospheric Environment*, 28, 1327-1338, 10.1016/1352-2310(94)90280-1, 1994.



- Jacobson, M.: Development and application of a new air pollution modeling system—II. Aerosol module structure and design, *Atmospheric Environment*, 31, 131-144, 10.1016/1352-2310(96)00202-6, 1997.
- 1055 Jimenez, J., Donahue, N., Prevot, A., Zhang, Q., Kroll, J., DeCarlo, P., Allan, J. D., Coe, H., Ng, N., Aiken, A., Docherty, K., Ulbrich, I., Grieshop, A., Robinson, A. L., Duplissy, J., Smith, J., Wilson, K., Lanz, V. A., and Worsnop, D.: Evolution of Organic Aerosols in the Atmosphere, *Science (New York, N.Y.)*, 326, 1525-1529, 10.1126/science.1180353, 2009.
- 1060 Kanakidou, M., Seinfeld, J., Pandis, S., Barnes, I., Dentener, F., Facchini, M., Van Dingenen, R., Ervens, B., Nenes, A., Nielsen, C., Swietlicki, E., Putaud, J.-P., Balkanski, Y., Sandro, F., Horth, J., Moortgat, G., Winterhalter, R., Lund Myhre, C., Tsigaridis, K., and Wilson, J.: Organic aerosol and global climate modelling: A review, *Journal of Atmospheric Chemistry*, 5, 1053-1123, 10.5194/acpd-4-5855-2004, 2005.
- 1065 Kelly, J. M., Doherty, R. M., O'Connor, F. M., and Mann, G. W.: The impact of biogenic, anthropogenic, and biomass burning volatile organic compound emissions on regional and seasonal variations in secondary organic aerosol, *Atmos. Chem. Phys.*, 18, 7393-7422, <https://doi.org/10.5194/acp-18-7393-2018>, 2018.
- 1070 Kirkby, J., Curtius, J., Almeida, J., Dunne, E., Duplissy, J., Ehrhart, S., Franchin, A., Gagné, S., Ickes, L., Kürten, A., Kupc, A., Metzger, A., Riccobono, F., Rondo, L., Schobesberger, S., Tsagkogeorgas, G., Wimmer, D., Amorim, A., Bianchi, F., and Kulmala, M.: Role of sulphuric acid, ammonia and galactic cosmic rays in atmospheric aerosol nucleation, *Nature*, 476, 429-433, 10.1038/nature10343, 2011.
- Koo, B., Knipping, E., and Yarwood, G.: 1.5-Dimensional volatility basis set approach for modeling organic aerosol in CAMx and CMAQ, *Atmospheric Environment*, 95, 158-164, 10.1016/j.atmosenv.2014.06.031, 2014.
- 1075 Kuang, C., McMurry, P. H., McCormick, A. V., and Eisele, F. L.: Dependence of nucleation rates on sulfuric acid vapor concentration in diverse atmospheric locations, *Journal of Geophysical Research Atmospheres*, 113, D10209, 10.1029/2007jd009253, 2008.
- 1080 Kuang, C., McMurry, P. H., and McCormick, A. V.: Determination of cloud condensation nuclei production from measured new particle formation events, 36, 10.1029/2009gl037584, 2009.
- Kulmala, M., Vehkamäki, H., Petaja, T., Dal Maso, M., Lauri, A., Kerminen, V.-M., Birmili, W., and McMurry, P.: Formation and growth rates of ultrafine atmospheric particles: A review of observations, *Journal of Aerosol Science*, 35, 176, 10.1016/j.jaerosci.2003.10.003, 2004.
- 1085 Kulmala, M., and Kerminen, V.-M.: On the formation and growth of atmospheric nanoparticles, *Atmospheric Research*, 90, 132-150, <https://doi.org/10.1016/j.atmosres.2008.01.005>, 2008.
- Kulmala, M., Kontkanen, J., Junninen, H., Lehtipalo, K., Manninen, H., Nieminen, T., Petäjä, T., Sipilä, M., Schobesberger, S., Rantala, P., Franchin, A., Jokinen, T., Järvinen, E., Äijälä, M., Kangasluoma, J., Hakala, J., Aalto, P., Paasonen, P., Mikkilä, J., and Worsnop, D.: Direct Observations of Atmospheric Aerosol Nucleation, *Science (New York, N.Y.)*, 339, 943-946, 10.1126/science.1227385, 2013.
- 1090 Kulmala, M., Petäjä, T., Kerminen, V.-M., Kujansuu, J., Ruuskanen, T., Ding, A., Nie, W., Hu, M., Wang, Z., Wu, Z., Wang, L., and Worsnop, D.: On secondary new particle formation in China, *Frontiers of Environmental Science & Engineering*, 10, 10.1007/s11783-016-0850-1, 2016.
- 1095



- Kulmala, M., Kerminen, V. M., Petaja, T., Ding, A. J., and Wang, L.: Atmospheric gas-to-particle conversion: why NPF events are observed in megacities?, *Faraday Discuss.*, 200, 271–288, <https://doi.org/10.1039/c6fd00257a>, 2017.
- 1100 Kumar, P., Morawska, L., Birmili, W., Paasonen, P., Hu, M., Kulmala, M., Harrison, R. M., Norford, L., and Britter, R.: Ultrafine particles in cities, *Environment international*, 66, 1-10, <https://doi.org/10.1016/j.envint.2014.01.013>, 2014.
- Lana, A., Bell, T., Simó, R., Vallina, S., Ballabrera, J., Kettle, A., Dachs, J., Bopp, L., Saltzman, E., Stefels, J., Johnson, J., and Liss, P.: An updated climatology of surface dimethylsulfide concentrations and emission fluxes in the global ocean, *Global Biogeochemical Cycles*, 25, 10.1029/2010GB003850, 2011.
- 1105 Lee, L. A., Pringle, K. J., Reddington, C. L., Mann, G. W., Stier, P., Spracklen, D. V., Pierce, J. R., and Carslaw, K. S.: The magnitude and causes of uncertainty in global model simulations of cloud condensation nuclei, *Atmos. Chem. Phys.*, 13, 8879–8914, <https://doi.org/10.5194/acp-13-8879-2013>, 2013.
- 1110 Li, J., Wang, Z., Zhuang, G., Luo, G., Sun, Y., and Wang, Q.: Mixing of Asian mineral dust with anthropogenic pollutants over East Asia: a model case study of a super-duststorm in March 2010, *Atmos. Chem. Phys.*, 12, 7591-7607, 10.5194/acp-12-7591-2012, 2012.
- Li, X.-L., Zhen, H., Wang, J.-S., Tu, X.-D., and Ye, C.: [Ultrafine particle number concentration and size distribution measurements in a street canyon], *Huan jing ke xue= Huanjing kexue / [bian ji, Zhongguo ke xue yuan huan jing ke xue wei yuan hui "Huan jing ke xue" bian ji wei yuan hui.]*, 28, 695-700, 2007a.
- 1115 Li, X., Wang, J., Tu, X., Liu, W., and Huang, Z.: Vertical variations of particle number concentration and size distribution in a street canyon in Shanghai, China, *The Science of the total environment*, 378, 306-316, 10.1016/j.scitotenv.2007.02.040, 2007b.
- 1120 Li, Y., Sun, Y., Zhang, Q., Li, X., Li, M., Zhou, Z., and Chan, C.: Real-time chemical characterization of atmospheric particulate matter in China: A review, *Atmospheric Environment*, 158, 10.1016/j.atmosenv.2017.02.027, 2017.
- Lin, G., Sillman, S., Penner, J. E., and Ito, A.: Global modeling of SOA: the use of different mechanisms for aqueous-phase formation, *Atmos. Chem. Phys.*, 14, 5451-5475, 10.5194/acp-14-5451-2014, 2014.
- 1125 Lin, J., An, J., Qu, Y., Chen, Y., Li, Y., Tang, Y., Wang, F., and Xiang, W.: Local and distant source contributions to secondary organic aerosol in the Beijing urban area in summer, *Atmospheric Environment*, 124, 176-185, <https://doi.org/10.1016/j.atmosenv.2015.08.098>, 2016.
- 1130 Liu, J., Horowitz, L., Fan, S.-M., Carlton, A. M., and Ii, L.: Global in-cloud production of secondary organic aerosols: Implementation of a detailed chemical mechanism in the GFDL atmospheric model AM3, *Journal of Geophysical Research (Atmospheres)*, 117, 15303, 10.1029/2012JD017838, 2012.
- 1135 Luo, G., and Wang, z.: A Global Environmental Atmospheric Transport Model(GEATM): Model Description and Validation, *Chinese Journal of Atmospheric Sciences*, 30, [https://doi.org/10.1016/S1003-6326\(06\)60040-X](https://doi.org/10.1016/S1003-6326(06)60040-X), 2006.
- Luo, G., and Yu, F.: Simulation of particle formation and number concentration over the Eastern United States with the WRF-Chem + APM model, *Atmospheric Chemistry and Physics Discussions*, 11, 14659-14688, 10.5194/acpd-11-14659-2011, 2011.



- 1140 Mann, G. W., Carslaw, K. S., Reddington, C. L., Pringle, K. J., Schulz, M., Asmi, A., Spracklen, D. V., Ridley, D. A., Woodhouse, M. T., Lee, L. A., Zhang, K., Ghan, S. J., Easter, R. C., Liu, X., Stier, P., Lee, Y. H., Adams, P. J., Tost, H., Lelieveld, J., Bauer, S. E., Tsigaridis, K., van Noije, T. P. C., Strunk, A., Vignati, E., Bellouin, N., Dalvi, M., Johnson, C. E., Bergman, T., Kokkola, H., von Salzen, K., Yu, F., Luo, G., Petzold, A., Heintzenberg, J., Clarke, A., Ogren, J. A., Gras, J., Baltensperger, U., Kaminski, U., Jennings, S. G., O'Dowd, C. D., Harrison, R. M., Beddows, D. C. S., Kulmala, M., Viisanen, Y., Ulevicius, V., Mihalopoulos, N., Zdimal, V., Fiebig, M., Hansson, H. C., Swietlicki, E., and Henzing, J. S.: Intercomparison and evaluation of global aerosol microphysical properties among AeroCom models of a range of complexity, *Atmos. Chem. Phys.*, 14, 4679-4713, 10.5194/acp-14-4679-2014, 2014.
- 1145 Matsui, H., Koike, M., Kondo, Y., Takami, A., Fast, J. D., Kanaya, Y., and Takigawa, M.: Volatility basis-set approach simulation of organic aerosol formation in East Asia: implications for anthropogenic–biogenic interaction and controllable amounts, *Atmos. Chem. Phys.*, 14, 9513–9535, <https://doi.org/10.5194/acp-14-9513-2014>, 2014.
- Matsui, H.: Development of a global aerosol model using a two-dimensional sectional method: 1. Model design: H. MATSUI: 2-D SECTIONAL GLOBAL AEROSOL MODEL 1, *Journal of Advances in Modeling Earth Systems*, 9, 10.1002/2017MS000936, 2017.
- 1155 May, A., Levin, E., Hennigan, C., Riipinen, I., Lee, T., Collett, J., Jimenez, J., Kreidenweis, S., and Robinson, A.: Gas-particle partitioning of primary organic aerosol emissions: 3. Biomass burning: BIOMASS-BURNING PARTITIONING, *Journal of Geophysical Research: Atmospheres*, 118, 10.1002/jgrd.50828, 2013a.
- 1160 May, A., Presto, A., Hennigan, C., Nguyễn, N. T., Gordon, T., and Robinson, A.: Gas-Particle Partitioning of Primary Organic Aerosol Emissions: (2) Diesel Vehicles, *Environmental science & technology*, 47, 10.1021/es400782j, 2013b.
- 1165 May, A. A., Presto, A. A., Hennigan, C. J., Nguyen, N. T., Gordon, T. D., and Robinson, A. L.: Gas-particle partitioning of primary organic aerosol emissions: (1) Gasoline vehicle exhaust, *Atmospheric Environment*, 77, 128-139, <https://doi.org/10.1016/j.atmosenv.2013.04.060>, 2013c.
- 1170 Metzger, A., Verheggen, B., Dommen, J., Duplissy, J., Prevot, A., Weingartner, E., Riipinen, I., Kulmala, M., Spracklen, D., Carslaw, K., and Baltensperger, U.: Evidence for the role of organics in aerosol particle formation under atmospheric conditions, *Proceedings of the National Academy of Sciences of the United States of America*, 107, 6646-6651, 10.1073/pnas.0911330107, 2010.
- 1175 Molteni, U., Bianchi, F., Klein, F., El Haddad, I., Frege, C., Rossi, M. J., Dommen, J., and Baltensperger, U.: Formation of highly oxygenated organic molecules from aromatic compounds, *Atmos. Chem. Phys.*, 18, 1909–1921, <https://doi.org/10.5194/acp-18-1909-2018>, 2018.
- Murphy, B., and Pandis, S.: Simulating the Formation of Semivolatile Primary and Secondary Organic Aerosol in a Regional Chemical Transport Model, *Environmental science & technology*, 43, 4722-4728, 10.1021/es803168a, 2009.
- 1180 Nenes, A., Pandis, S., and Pilinis, C.: ISORROPIA: A New Thermodynamic Equilibrium Model for Multiphase Multicomponent Inorganic Aerosols, *Aquatic Geochemistry*, 4, 123-152, 10.1023/A:1009604003981, 1998.



- 1185 Odum, J., Hoffmann, T., Bowman, F., Collins, D., Flagan, R., and Seinfeld, J.: Gas/Particle Partitioning and Secondary Organic Aerosol Yields, *Environmental science & technology*, 30, 10.1021/es950943+, 1996.
- Pankow, J.: An absorption model of gas/particle partitioning of organic compounds in the atmosphere, *Atmospheric Environment*, 28, 185-188, 10.1016/1352-2310(94)90093-0, 1994a.
- 1190 Pankow, J. F.: An absorption model of the gas/aerosol partitioning involved in the formation of secondary organic aerosol, *Atmospheric Environment*, 28, 189-193, 10.1016/j.atmosenv.2007.10.060, 1994b.
- Patoulias, D., Fountoukis, C., Riipinen, I., and Pandis, S. N.: The role of organic condensation on ultrafine particle growth during nucleation events, *Atmos. Chem. Phys.*, 15, 6337-6350, 10.5194/acp-15-6337-2015, 2015.
- 1195 Paasonen P, Visshedjik A, Kupiainen K, Klimont Z, van der Gon HD, KulmalaM, et al. Aerosolparticle number emissions and size distributions: implementation in the GAINSmodel and initial results. IIASA interim report; 2013.
- Pierce, J., Riipinen, I., Kulmala, M., Ehn, M., Petäjä, T., Junninen, H., Worsnop, D., and Donahue, N.: Quantification of the volatility of secondary organic compounds in ultrafine particles during nucleation events, *Atmospheric Chemistry and Physics*, 11, 1200 10.5194/acp-11-9019-2011, 2011.
- Reddington, C., McMeeking, G., Mann, G., Coe, H., Frontoso, M., Liu, D., Flynn, M., Spracklen, D., and Carslaw, K.: The mass and number size distributions of black carbon aerosol over Europe, *Atmospheric Chemistry & Physics*, 13, 4917-4939, 10.5194/acp-13-4917-2013, 1205 2013.
- Riipinen, I., Pierce, J., Yli-Juuti, T., Nieminen, T., Häkkinen, S., Ehn, M., Junninen, H., Lehtipalo, K., Petäjä, T., Slowik, J., Chang, R., Shantz, N., Abbatt, J., Leaitch, W., Kerminen, V.-M., Worsnop, D., Pandis, S., Donahue, N., and Kulmala, M.: Organic condensation: A vital link connecting aerosol formation to cloud condensation nuclei (CCN) concentrations, *Atmospheric Chemistry & Physics*, 11, 3865-3878, 10.5194/acp-11-3865-2011, 2011. 1210
- Robinson, A., Donahue, N., Shrivastava, M., Weitkamp, E., Sage, A., Grieshop, A., Lane, T., Pierce, J., and Pandis, S.: Rethinking Organic Aerosols: Semivolatile Emissions and Photochemical Aging, *Science (New York, N.Y.)*, 315, 1259-1262, 10.1126/science.1133061, 2007.
- 1215 Seinfeld, J., and Pandis, S.: *Atmospheric Chemistry and Physics: From Air Pollution to Climate Change*, in, 1998.
- Seinfeld J H, Pandis S N. *Atmospheric Chemistry and Physics: From Air Pollution to Climate Change*[M]. New York: John Wiley & Sons, Inc., 2006.
- 1220 Sheehan, P., and Bowman, F.: Estimated Effects of Temperature on Secondary Organic Aerosol Concentrations, *Environmental science & technology*, 35, 2129-2135, 10.1021/es001547g, 2001.
- Shrivastava, M., Donahue, N., Pandis, S., and Robinson, A.: Effects of gas particle partitioning and aging of primary emissions on urban and regional organic aerosol concentrations, *Journal of Geophysical Research*, 113, 10.1029/2007JD009735, 2008.
- 1225 Shrivastava, M., Cappa, C. D., Fan, J., Goldstein, A. H., Guenther, A. B., Jimenez, J. L., Kuang, C., Laskin, A., Martin, S. T., Ng, N. L., Petaja, T., Pierce, J. R., Rasch, P. J., Roldin, P.,



- 1230 Seinfeld, J. H., Shilling, J., Smith, J. N., Thornton, J. A., Volkamer, R., Wang, J., Worsnop, D. R., Zaveri, R. A., Zelenyuk, A., and Zhang, Q.: Recent advances in understanding secondary organic aerosol: Implications for global climate forcing, *Reviews of Geophysics*, 55, 509-559, 10.1002/2016rg000540, 2017.
- Skamarock, W., Klemp, J.B., Dudhia, J., Gill, D.O., Barker, D., 2008. A Description of the Advanced Research WRF Version 3. NCAR Technical Note NCAR/TN- 475tSTR.
- 1235 Spracklen, D., Pringle, K., Carslaw, K., Chipperfield, M., and Mann, G.: A global off-line model of size-resolved aerosol microphysics: I. Model development and prediction of aerosol properties, *Atmospheric Chemistry and Physics*, 5, 10.5194/acp-5-2227-2005, 2005.
- Spracklen, D. V., Carslaw, K. S., Kulmala, M., Kerminen, V.-M., Mann, G. W., and Sihto, S.-L.: The contribution of boundary layer nucleation events to total particle concentrations on regional and global scales, *Atmos. Chem. Phys.*, 6, 5631-5648, <https://doi.org/10.5194/acp-6-5631-2006>, 2006.
- 1240 Spracklen, D., Carslaw, K., Kulmala, M., Kerminen, V.-M., Sihto, S.-L., Riipinen, I., Merikanto, J., Mann, G., Chipperfield, M., Wiedensohler, A., Birmili, W., and Lihavainen, H.: Contribution of particle formation to global cloud condensation nuclei concentrations, *Geophysical Research Letters - GEOPHYS RES LETT*, 35, 10.1029/2007GL033038, 2008.
- 1245 Spracklen, D., Carslaw, K., Merikanto, J., Mann, G., Reddington, C., Pickering, S., Ogren, J., Andrews, E., Baltensperger, U., Weingartner, E., Boy, M., Kulmala, M., Laakso, L., Lihavainen, H., Kivekäs, N., Komppula, M., Mihalopoulos, N., Kouvarakis, G., Jennings, S., and Sun, J.: Explaining global surface aerosol number concentrations in terms of primary emissions and particle formation, *Atmospheric Chemistry and Physics*, 10, 10.5194/acp-10-4775-2010, 2010.
- 1250 Spracklen, D., Jimenez, J., Carslaw, K., Worsnop, D., Evans, M., Mann, G., Zhang, Q., Allan, J., Coe, H., McFiggans, G., Rap, A., and Forster, P.: Aerosol mass spectrometer constraint on the global secondary organic aerosol budget, *Atmospheric Chemistry and Physics*, 11, 10.5194/acp-11-12109-2011, 2011.
- 1255 Spracklen, D. V., Carslaw, K. S., Kulmala, M., Kerminen, V. M., Mann, G. W., and Sihto, S. L.: The contribution of boundary layer nucleation events to total particle concentrations on regional and global scales, *Atmos. Chem. Phys.*, 6, 5631-5648, 10.5194/acp-6-5631-2006, 2006.
- 1260 Stier, P., Feichter, J., Kinne, S., Kloster, S., Vignati, E., Wilson, J., Ganzeveld, L., Tegen, I., Werner, M., Balkanski, Y., Michael, S., Boucher, O., Minikin, A., and Petzold, A.: The aerosol-climate model ECHAM5-HAM, *Atmospheric Chemistry and Physics*, v.5, 1125-1156 (2005), 5, 10.5194/acp-5-1125-2005, 2005.
- Stockwell, W., Middleton, P., and Chang, J.: The Second Generation Regional Acid Deposition Model Chemical Mechanism for Regional Air Quality Modeling, *Journal of Geophysical Research*, 951, 16343-16367, 10.1029/JD095iD10p16343, 1990.
- 1265 Sun, Y., Wang, Z., Du, W., Zhang, Q., Wang, Q., Fu, P., Pan, X., Li, J., Jayne, J., and Worsnop, D.: Long-term real-time measurements of aerosol particle composition in Beijing, China: Seasonal variations, meteorological effects, and source analysis, *Atmospheric Chemistry and Physics*, 15, 10149-10165, 10.5194/acp-15-10149-2015, 2015.



- 1270 Tang, R., Wu, Z., Li, X., Wang, Y., Shang, D., Xiao, Y., Li, M., Zeng, L., Wu, Z., Hallquist, M.,  
Hu, M., and Guo, S.: Primary and secondary organic aerosols in summer 2016 in Beijing,  
Atmos. Chem. Phys., 18, 4055–4068, 10.5194/acp-18-4055-2018, 2018.
- Trivitanurak, W. and Adams, P. J.: Does the POA–SOA split matter for global CCN formation?,  
Atmos. Chem. Phys., 14, 995–1010, <https://doi.org/10.5194/acp-14-995-2014>, 2014.
- 1275 Tröstl, J., Chuang, W., Gordon, H., Heinritzi, M., Yan, C., Molteni, U., Ahlm, L., Frege, C.,  
Bianchi, F., Wagner, R., Simon, M., Lehtipalo, K., Williamson, C., Craven, J., Duplissy, J.,  
Adamov, A., Almeida, J., Bernhammer, A.-K., Breitenlechner, M., and Baltensperger, U.:  
The role of low-volatility organic compounds in initial particle growth in the atmosphere,  
Nature, 533, 2016.
- 1280 Tsigaridis, K., Krol, M., Dentener, F. J., Balkanski, Y., Lathière, J., Metzger, S., Hauglustaine, D.  
A., and Kanakidou, M.: Change in global aerosol composition since preindustrial times,  
Atmos. Chem. Phys., 6, 5143–5162, 10.5194/acp-6-5143-2006, 2006.
- 1285 Tsigaridis, K., Daskalakis, N., Kanakidou, M., Adams, P., Artaxo, P., Bahadur, R., Balkanski, Y.,  
Bauer, S., Bellouin, N., Benedetti, A., Bergman, T., Berntsen, T., Beukes, J., Bian, H.,  
Carslaw, K., Chin, M., Curci, G., Diehl, T., Easter, R., and Zhang, X.: The AeroCom  
evaluation and intercomparison of organic aerosol in global models, Atmospheric Chemistry  
and Physics Discussions, 14, 10.5194/acpd-14-6027-2014, 2014.
- Twomey, S.: The Influence of Pollution on the Shortwave Albedo of Clouds, Journal of The  
Atmospheric Sciences - J ATMOS SCI, 34, 1149–1154,  
10.1175/1520-0469(1977)034<1149:TlOPOT>2.0.CO;2, 1977.
- 1290 Ulbrich, I., Zhang, Q., Worsnop, D., and Jimenez, J.: Interpretation of organic components from  
Positive Matrix Factorization of aerosol mass spectrometric data, Atmospheric Chemistry and  
Physics Discussions, 9, 10.5194/acp-9-2891-2009, 2008.
- 1295 Ulrike, D., Frank, G., Hildebrandt Ruiz, L., Curtius, J., Schneider, J., Walter, S., Chand, D.,  
Drewnick, F., Hings, S., Jung, D., Borrmann, S., and Andreae, M.: Size Matters More Than  
Chemistry for Cloud-Nucleating Ability of Aerosol Particles, Science (New York, N.Y.), 312,  
1375–1378, 10.1126/science.1125261, 2006.
- Walcek, C., and Aleksic, N.: A simple but accurate mass conservative, peak-preserving, mixing  
ratio bounded advection algorithm with FORTRAN code, Atmospheric Environment, 32,  
3863–3880, 10.1016/S1352-2310(98)00099-5, 1998.
- 1300 Wang, H., Chen, H., Wu, Q., Lin, J., Chen, G., Xie, X., Wang, R., Tang, X., and Wang, Z.:  
GNAQPMS v1.1: accelerating the Global Nested Air Quality Prediction Modeling System  
(GNAQPMS) on Intel Xeon Phi processors, Geoscientific Model Development, 10,  
2891–2904, 10.5194/gmd-10-2891-2017, 2017.
- 1305 Wang, H., Lin, J., Wu, Q., Chen, H., Tang, X., Wang, Z., Chen, G., Cheng, H., and Wang, L.: MP  
CBM-Z V1.0: Design for a new Carbon Bond Mechanism Z (CBM-Z) gas-phase chemical  
mechanism architecture for next-generation processors, Geoscientific Model Development,  
12, 749–764, 10.5194/gmd-12-749-2019, 2019.
- 1310 Wang, Z., Ueda, H., and Huang, M.: A deflation module for use in modeling long-range transport  
of yellow sand over East Asia, Journal of Geophysical Research, 105, 26947–26960,  
10.1029/2000JD900370, 2000.



- Wang, Z., Maeda, T., Hayashi, M., Hsiao, L. F., and Liu, K. Y.: A Nested Air Quality Prediction Modeling System for Urban and Regional Scales: Application for High-Ozone Episode in Taiwan, *Water Air and Soil Pollution*, 130, 391-396, 10.1023/A:1013833217916, 2001.
- 1315 Wang, Z., Hu, M., Wu, Z., and Yue, D.: Research on the Formation Mechanisms of New Particles in the Atmosphere, *Acta Chimica Sinica*, 71, 519, 10.6023/A12121062, 2013.
- Wang, Z., Wu, Z., Yue, D., Shang, D., Guo, S., Sun, J., Ding, A., Wang, L., Jiang, J., Guo, H., Gao, J., Cheung, H. C., Morawska, L., Keywood, M., and Hu, M.: New particle formation in China: Current knowledge and further directions, *Science of The Total Environment*, 577, 10.1016/j.scitotenv.2016.10.177, 2016.
- 1320 Wang, Z. B., Hu, M., Pei, X., Zhang, R. Y., Paasonen, P., Zheng, J., Yue, D. L., Wu, Z., Boy, M., and Wiedensohler, A.: Connection of organics to atmospheric new particle formation and growth at an urban site of Beijing, *Atmospheric Environment*, 103, 10.1016/j.atmosenv.2014.11.069, 2015.
- 1325 Wehner, B., Wiedensohler, A., Tuch, T., Wu, Z., Hu, M., Slanina, J., and Kiang, C.: Variability of the Aerosol Number Size Distribution in Beijing, China: New Particle Formation, Dust Storms, and High cContinental Background, *Geophysical Research Letters - GEOPHYS RES LETT*, 31, 10.1029/2004GL021596, 2004.
- 1330 Wei, Y., Chen, X., Chen, H., Li, J., Wang, Z., Yang, W., Ge, B., Du, H., Hao, J., Wang, W., Li, J., Sun, Y., and Huang, H.: IAP-AACM v1.0: a global to regional evaluation of the atmospheric chemistry model in CAS-ESM, *Atmos. Chem. Phys.*, 19, 8269-8296, 10.5194/acp-19-8269-2019, 2019.
- 1335 Wiedensohler, A., Cheng, Y., Nowak, A., Wehner, B., Achtert, P., Berghof, M., Birmili, W., Wu, Z., Hu, M., Zhu, T., Takegawa, N., Kita, K., Kondo, Y., Lou, S., Hofzumahaus, A., Holland, F., Wahner, A., Gunthe, S., Rose, D., and Pöschl, U.: Rapid aerosol particle growth and increase of cloud condensation nucleus activity by secondary aerosol formation and condensation: A case study for regional air pollution in northeastern China, *Journal of Geophysical Research-Atmospheres*, v.114 (2009), 114, 10.1029/2008JD010884, 2009.
- 1340 Wu, Z., Hu, M., Liu, S., Wehner, B., Bauer, S., Ssling, A., Wiedensohler, A., Petäjä, T., Dal Maso, M., and Kulmala, M.: New particle formation in Beijing, China: Statistical analysis of a 1-year data set, *Journal of Geophysical Research (Atmospheres)*, 112, 9209, 10.1029/2006JD007406, 2007.
- Wu, Z., Hu, M., Lin, P., Liu, S., Wehner, B., and Wiedensohler, A.: Particle number size distribution in the urban atmosphere of Beijing, China, *Atmospheric Environment*, 42, 7967-7980, 10.1016/j.atmosenv.2008.06.022, 2008.
- 1345 Xausa, F., Paasonen, P., Makkonen, R., Arshinov, M., Ding, A., Denier Van Der Gon, H., Kerminen, V.-M., and Kulmala, M.: Advancing global aerosol simulations with size-segregated anthropogenic particle number emissions, *Atmos. Chem. Phys.*, 18, 10039–10054, <https://doi.org/10.5194/acp-18-10039-2018>, 2018.
- 1350 Xu, W., Xie, C., Karnezi, E., Zhang, q., Wang, J., Pandis, S., ge, X., Zhang, J., An, J., Wang, Q., Zhao, J., Du, W., Qiu, Y., Zhou, W., He, Y., Li, Y., Li, J., Fu, P., Wang, Z., and Sun, Y.: Summertime aerosol volatility measurements in Beijing, China, *Atmospheric Chemistry and Physics*, 19, 10205-10216, 10.5194/acp-19-10205-2019, 2019.



- 1355 Yang, F., Kawamura, K., Chen, J., Ho, K. F., Lee, S., Gao, Y., Cui, L., Wang, T., and Fu, P.: Anthropogenic and biogenic organic compounds in summertime fine aerosols (PM<sub>2.5</sub>) in Beijing, China, *Atmospheric Environment*, 10.1016/j.atmosenv.2015.08.095, 2016.
- Yang, W., Li, J., Wang, W., Li, J., Ge, M.-F., Sun, Y., Chen, G., Ge, B., Tong, S., Wang, Q., and Wang, Z.: Investigating secondary organic aerosol formation pathways in China during 2014, *Atmospheric Environment*, 213, 10.1016/j.atmosenv.2019.05.057, 2019.
- 1360 Yao, L., Garmash, O., Bianchi, F., Zheng, J., Yan, C., Kontkanen, J., Junninen, H., Mazon, S., Ehn, M., Paasonen, P., Sipilä, M., Wang, M., Wang, X., Xiao, S., Chen, H., Lu, Y., Zhang, B., Wang, D., Fu, Q., and Wang, L.: Atmospheric new particle formation from sulfuric acid and amines in a Chinese megacity, *Science*, 361, 278-281, 10.1126/science.aao4839, 2018.
- 1365 Yu, F., and Turco, R.: From molecular clusters to nanoparticles: Role of ambient ionization in tropospheric aerosol formation, *Journal of Geophysical Research*, 106, 4797-4814, 10.1029/2000JD900539, 2001.
- Yu, F.: From molecular clusters to nanoparticles: Second-generation ion-mediated nucleation model, *Atmospheric Chemistry and Physics*, 6, 10.5194/acp-6-5193-2006, 2006.
- Yu, F., Wang, Z., and Turco, R.: Ion-mediated Nucleation as an Important Source of Global Tropospheric Aerosols, in, 938-942, 2007.
- 1370 Yu, F., and Luo, G.: Simulation of particle size distribution with a global aerosol model: Contribution of nucleation to aerosol and CCN number concentrations, *Atmospheric Chemistry and Physics Discussions*, 9, 10.5194/acpd-9-10597-2009, 2009.
- Yu, F.: Ion-mediated nucleation in the atmosphere: Key controlling parameters, implications, and look-up table, *Journal of Geophysical Research*, 115, 10.1029/2009JD012630, 2010.
- 1375 Yu, F.: A secondary organic aerosol formation model considering successive oxidation aging and kinetic condensation of organic compounds: Global scale implications, *Atmospheric Chemistry and Physics*, 11, 10.5194/acp-11-1083-2011, 2011.
- 1380 Yu, F., Nadykto, A., Herb, J., Luo, G., Nazarenko, K., and Uvarova, L.: H<sub>2</sub>SO<sub>4</sub>-H<sub>2</sub>O-NH<sub>3</sub> ternary ion-mediated nucleation (TIMN): Kinetic-based model and comparison with CLOUD measurements, *Atmospheric Chemistry and Physics Discussions*, 1-41, 10.5194/acp-2018-396, 2018.
- 1385 Yue, D. L., Hu, M., Zhang, R. Y., Wu, Z., Su, H., Wang, Z. B., Peng, J., He, L. Y., Huang, X., Gong, Y. G., and Wiedensohler, A.: Potential contribution of new particle formation to cloud condensation nuclei in Beijing, *Atmospheric Environment*, 45, 6070-6077, 10.1016/j.atmosenv.2011.07.037, 2011.
- Zaveri, R., and Peters, L.: A new lumped structure photochemical mechanism for long-scale applications, *Journal of Geophysical Research*, 104, 30387-30415, 10.1029/1999JD900876, 1999.
- 1390 Zhang, L., Brook, J., and R, V.: A revised parameterization for gaseous dry deposition in air-quality models, *Atmospheric Chemistry and Physics*, 3, 10.5194/acpd-3-1777-2003, 2003.
- Zhang, Q., Jimenez, J., Allan, J., Coe, H., Ulbrich, I., Alfarra, M., Takami, A., Middlebrook, A., Sun, Y. L., Dzepina, K., Dunlea, E., Docherty, K., DeCarlo, P., Salcedo, D., Onasch, T., Jayne, J., Miyoshi, T., Shimojo, A., and Worsnop, D.: Ubiquity and dominance of oxygenated species in organic aerosols in anthropogenically-influenced Northern Hemisphere midlatitudes, *Geophysical Research Letters*, v.34 (2007), 34, L13801, 10.1029/2007GL029979, 2013.



- Zhang, R., Khalizov, A., Wang, L., Hu, M., and Xu, W.: Nucleation and Growth of Nanoparticles in the Atmosphere, *Chemical reviews*, 112, 1957-2011, 10.1021/cr2001756, 2011.
- 1400 Zhang, X., Wang, Y., Zhang, X., Guo, W., and Gong, S.: Carbonaceous aerosol composition over various regions of China during 2006, *Journal of Geophysical Research*, 113, 10.1029/2007JD009525, 2008.
- Zhang, Y., Liu, P., Liu, X.-H., Jacobson, M., McMurry, P., Yu, F., Yu, S., and Schere, K.: A comparative study of nucleation parameterizations: 2. Three-dimensional model application and evaluation, *Journal of Geophysical Research*, 115, 10.1029/2010JD014151, 2010.
- 1405 Zhao, B., Wang, S., Donahue, N., Jathar, S., Huang, X., Wu, W., Hao, J., and Robinson, A.: Quantifying the effect of organic aerosol aging and intermediate-volatility emissions on regional-scale aerosol pollution in China, *Scientific reports*, 6, 10.1038/srep28815, 2016a.
- Zhao, J., Du, W., Zhang, Y., Wang, Q., Chen, C., Xu, W., Han, T., Yuying, W., Fu, P., Wang, Z., Li, z., and Sun, Y.: Insights into Aerosol Chemistry during the 2015 China Victory Day  
1410 Parade: Results from Simultaneous Measurements at Ground Level and 260 m in Beijing, *Atmospheric Chemistry and Physics Discussions*, 1-29, 10.5194/acp-2016-695, 2016b.
- Zhou, C., Gong, S., Zhang, X.-Y., Liu, H.-L., Xue, M., Cao, G.-L., An, X.-Q., Che, H., Zhang, Y.-M., and Niu, T.: Towards the improvements of simulating the chemical and optical  
1415 properties of Chinese aerosols using an online coupled model CUACE/Aero, *Tellus B*, 64, 10.3402/tellusb.v64i0.18965, 2012.
- Zhou, C., Shen, X., Liu, Z., Zhang, Y., and Xin, J.: Simulating Aerosol Size Distribution and Mass Concentration with Simultaneous Nucleation, Condensation/Coagulation, and Deposition with the GRAPES-CUACE, *Journal of Meteorological Research*, 32, 265-278, 10.1007/s13351-018-7116-8, 2018.
- 1420 Zhu, J., Penner, J. E., Lin, G., Zhou, C., Xu, L., and Zhuang, B.: Mechanism of SOA formation determines magnitude of radiative effects, *Proceedings of the National Academy of Sciences of the United States of America*, 114, 12685-12690, 10.1073/pnas.1712273114, 2017.